Received: 29 December 2020 | Revised: 1 June 2021 | Accepted: 8 June 2021

DOI: 10.1111/bph.15600

RESEARCH ARTICLE

Activation of AMP kinase ameliorates kidney vascular dysfunction, oxidative stress and inflammation in rodent models of obesity

Claudia Rodríguez[1] | Ana Sánchez[1] | Javier Sáenz-Medina[2] | Mercedes Muñoz[1] | Medardo Hernández[1] | Miguel López[3] | Luis Rivera[1] | Cristina Contreras[1] | Dolores Prieto[1]

[1]Departamento de Fisiología, Facultad de Farmacia, Universidad Complutense, Madrid, Spain

[2]Departamento de Urología, Hospital Universitario Puerta de Hierro-Majadahonda, Madrid, Spain

[3]NeurObesity Group, Department of Physiology, CIMUS, Universidad de Santiago de Compostela-Instituto de Investigación Sanitaria, Santiago de Compostela, Spain

Correspondence
Dolores Prieto, Departamento de Fisiología, Facultad de Farmacia, Universidad Complutense de Madrid, 28040 Madrid, Spain.
Email: dprieto@ucm.es

Funding information
Ministerio de Ciencia e Innovación (Spain), Grant/Award Numbers: PID2019-105689RB, RTI2018-101840-B-I00; Ministerio de Economía y Competitividad (Spain), Grant/Award Number: SAF2016-77526-R

Background and Purpose: Obesity is a risk factor for the development of chronic kidney disease independent of diabetes, hypertension and other co-morbidities. Obesity-associated nephropathy is linked to dysregulation of the cell energy sensor AMP-activated protein kinase (AMPK). We aimed here to assess whether impairment of AMPK activity may cause renal arterial dysfunction in obesity and to evaluate the therapeutic potential of activating renal AMPK.

Experimental Approach: Effects of the AMPK activator A769662 were assessed on intrarenal arteries isolated from *ob/ob* mice and obese Zucker rats and then mounted in microvascular myographs. Superoxide and hydrogen peroxide production were measured by chemiluminescence and fluorescence, respectively, and protein expression was analysed by western blotting.

Key Results: Endothelium-dependent vasodilation and PI3K/Akt/eNOS pathway were impaired in preglomerular arteries from genetically obese rats and mice, along with impaired arterial AMPK activity and blunted relaxations induced by the AMPK activator A769662. Acute ex vivo exposure to A769662 restored endothelial function and enhanced activity of PI3K/Akt/eNOS pathway in obese rats, whereas in vivo treatment with A769662 improved metabolic state and ameliorated endothelial dysfunction, reduced inflammatory markers and vascular oxidative stress in renal arteries and restored redox balance in renal cortex of obese mice.

Conclusion and Implications: These results demonstrate that AMPK dysregulation underlies obesity-associated kidney vascular dysfunction and activation of AMPK improves metabolic state, protects renal endothelial function and exerts potent vascular antioxidant and anti-inflammatory effects. The beneficial effects of vascular

Abbreviations: ACC, acetyl-CoA carboxylase; AMPK, AMP-activated protein kinase; CKD, chronic kidney disease; EC, endothelial cell; EDH, endothelium-derived-hyperpolarization; eNOS, endothelial NOS; ER, endoplasmic reticulum; IK_{Ca} channel, intermediate-conductance calcium-activated K + channel; IKK, IκB kinase; K_{ATP}, ATP-sensitive potassium channels; LZR, lean Zucker rats; NADPH, nicotinamide adenine dinucleotide phosphate; Nox4, NADPH oxidase 4; OZR, obese Zucker rats; PSS, physiological saline solution; SERCA, sarcoplasmic reticulum Ca^{2+}-ATPase; SR, sarcoplasmic reticulum; VSM, vascular smooth muscle.

This is an open access article under the terms of the Creative Commons Attribution-NonCommercial-NoDerivs License, which permits use and distribution in any medium, provided the original work is properly cited, the use is non-commercial and no modifications or adaptations are made.
© 2021 The Authors. *British Journal of Pharmacology* published by John Wiley & Sons Ltd on behalf of British Pharmacological Society.

AMPK activation might represent a promising therapeutic approach to the treatment of obesity-related kidney injury.

KEYWORDS
AMPK, endothelial dysfunction, inflammation, kidney, obesity, oxidative stress

1 | INTRODUCTION

Obesity has become a public health problem of increasing prevalence worldwide due to an increase in sedentary lifestyles and excess caloric intake. Obesity and metabolic syndrome are associated with an increased risk of diabetic complications including diabetic nephropathy and chronic kidney disease (CKD) (Abrass, 2004). However, obese non-diabetic individuals can also develop CKD and epidemiological data show that obesity is a risk factor for CKD independent of diabetes, hypertension and other co-morbidities (De Vries et al., 2014; Kramer et al., 2005). Obesity-related kidney injury has been associated with structural abnormalities such as glomerular hypertrophy, tubular injury and tubulointerstitial fibrosis that lead to progressive impairment of renal function and microalbuminuria, proteinuria, glomerular hyperfiltration, endothelial and podocyte dysfunction and abnormal renal haemodynamics (Amann & Benz, 2013; De Vries et al., 2014; Sharma, 2014). The pathogenic mechanisms proposed to link kidney disease and obesity include renal lipid accumulation and lipotoxicity, proinflammatory changes, abnormal secretion of adipokines, endothelial dysfunction, hypertension and oxidative stress (Amann & Benz, 2013; De Vries et al., 2014; Muñoz et al., 2015, 2018).

The enzyme AMP kinase (**AMPK**) is a key cellular energy sensor that is activated in response to ATP depletion (increased AMP/ATP ratio) in energy deficiency states and stimulates catabolic pathways to restore energy homeostasis. AMPK is abundantly expressed in the kidney (Decleves et al., 2014; Hallows et al., 2010), a highly energy-consuming organ, and its activation plays an important role in the regulation of glucose and fatty acid (FA) metabolism, ion transport and podocyte function (Hallows et al., 2010). Furthermore, activation of vascular AMPK in the kidney has recently been identified by our group as a new physiological target that induces renal vasodilation through endothelium-dependent and independent mechanisms and down-regulates ROS production under physiological conditions (Rodríguez et al., 2020). Therefore, modulation of renal blood flow and vasodilation by AMPK activation may facilitate cellular nutrient uptake to restore energy levels dependent on the state of kidney metabolism.

AMPK dysregulation has been reported under conditions of metabolic stress such as obesity and diabetes, and also in vascular disorders and CKD (Decleves et al., 2011; Dugan et al., 2013; Ruderman & Prentki, 2004; Steinberg & Kemp, 2009). At a central level, hypothalamic AMPK integrates peripheral signals to regulate feeding behaviour and thermogenesis, and augmented AMPK activity increases feeding while decreasing thermogenesis, thus worsening metabolic states in obesity (Lopez et al., 2016). In contrast, overnutrition and metabolic stress induced by obesity are linked to reduced-AMPK activity and dysregulation of lipid metabolism in peripheral organs including kidney (Declèves & Sharma, 2015). AMPK phosphorylates acetyl-CoA carboxylase (**ACC**) to increase β-oxidation of fatty acids and to decrease lipid synthesis. Decreased activity of AMPK and p-ACC leads to impairment of lipid oxidation by mitochondria in the diabetic kidney (Decleves et al., 2014; Dugan et al., 2013). AMPK dysregulation has also been associated with glomerulopathy, enhanced profibrotic pathways (**TGF-β1** and mesangial matrix expansion) and lipotoxicity-induced proximal tubule injury in high fat diet models of obesity (Decleves et al., 2011, 2014). Furthermore, oxidative stress and inflammation have been linked to AMPK dysregulation in the obese kidney because activation of AMPK was beneficial in reducing inflammation markers and ROS production in renal tissues (Dugan et al., 2013; Sharma, 2014, 2016).

What is already known

- Obesity is a risk factor for chronic kidney disease independent of diabetes and hypertension.
- AMPK dysregulation has been associated with glomerulopathy, fibrosis and lipotoxicity-induced tubule injury in obesity-associated nephropathy.

What does this study add

- Reduced vascular AMPK activity was associated with endothelial dysfunction, oxidative stress and inflammation in obesity.
- AMPK activation with A769662 improved metabolic state, ameliorated endothelial dysfunction, oxidative stress and inflammation.

What is the clinical significance

- Vascular AMPK dysregulation may be involved in the pathogenesis of obesity-associated kidney injury.
- Vascular AMPK activation should be considered as a therapeutic target for treatment of metabolic disease-related-nephropathy.

Impaired AMPK vascular activity has been involved in the development of obesity-associated endothelial dysfunction (García-Prieto, Hernández-Nuño, et al., 2015; García-Prieto, Pulido-Olmo, et al., 2015; Lee et al., 2005; Lobato et al., 2013), a hallmark of metabolic disease vascular complications (Prieto et al., 2014). Hence, drugs such as metformin, commonly used in the treatment of diabetes, have been shown to exert cardiovascular protection through activation of vascular AMPK (Calvert et al., 2008; Ewart & Kennedy, 2011; García-Prieto, Gil-Ortega, et al., 2015), resulting in augmented endothelial NO production (Deng et al., 2010; Rossoni et al., 2011; Sun et al., 2006; Zhou et al., 2001). The hypothesis of the present study is that vascular AMPK dysregulation is involved in renal endothelial dysfunction and therefore might affect renal function and contribute to obesity-associated kidney injury. Therefore, activation of kidney vascular AMPK could be a potential therapeutic target against nephropathy associated with metabolic disease (Salatto et al., 2017).

2 | METHODS

2.1 | Animal models

All animal care and experimental protocols conformed to the European Union Directive 2010/63/EU on the Protection of Animals Used for Scientific Purposes and were approved by the Institutional Animal Care and Use Committee of Madrid Complutense University and Comunidad de Madrid (PROEX109/16). All animal experiments are reported in compliance with the ARRIVE guidelines (Percie du Sert et al., 2020) and with the recommendations made by the *British Journal of Pharmacology* (Lilley et al., 2020).

Male obese Zucker rats (OZR, fa/fa) and their counterparts lean Zucker rats (LZR, fa/−) were purchased from Charles River Laboratories (Madrid, Spain), and *ob/ob* mice (obese B6.V-Lep$^{ob/ob}$/JRj) and their lean littermates were purchased from Janvier Labs (Madrid, Spain). These animals were used as models of genetic obesity/metabolic syndrome at 17–19 weeks (rats) and 11–13 weeks of age (mice). The fa mutation in the OZR is an autosomal recessive locus on chromosome 5, and homogeneity results in an improperly coded leptin receptor gene leading to hyperphagia, obesity, hyperinsulinaemia and poor glucose tolerance although the animals are not overtly diabetic. The *ob/ob* mice are homozygous for the obese spontaneous mutation Lep*ob* and exhibit obesity, hyperphagia, transient hyperglycaemia, glucose intolerance and elevated plasma insulin. Male rats/mice were used because they are not subject to cyclical hormonal changes. Animals were housed at Complutense University, Pharmacy School animal care facility in separate rooms. Animals were maintained on standard chow and water ad libitum, under controlled temperature (23 ± 1°C) and humidity (40%–60%) and a 12:12 hr light/dark cycle. Animals were killed under CO_2 anaesthesia by decapitation. Then, kidneys, mesentery or heart were quickly removed and placed in cold physiological saline solution (PSS) of the following composition (mM): NaCl 119, $NaHCO_3$ 25, KCl 4.7, KH_2PO_4 1.17, $MgSO_4$ 1.18, $CaCl_2$ 1.5, EDTA 0.027 and glucose 11.

Pharmacological experiments to assess the effects of AMPK activation on endothelial function, vascular ROS generation and expression of proteins of the AMPK/ACC and Akt/eNOS signalling pathways were carried out ex vivo in isolated renal arteries from OZR, compared with LZR controls. To evaluate the in vivo effects of AMPK activation on renal vascular dysfunction in obesity, large amounts of A769662 were required for treatment in rats, and interlobar renal arteries from the *ob/ob* mouse model of genetic obesity were used to study the effects of the AMPK activation. Because adequate amounts of tissue could not be obtained in this model to run ROS measurements and western blot analysis in arteries, renal cortex samples were used in parallel with myograph experiments in arteries.

2.2 | In vivo studies

For the in vivo experiments, *ob/ob* ($n = 12$) and lean mice ($n = 12$) were individually housed for daily food-intake and body weight measurements and randomly separated into four experimental groups for a 4-day study with six animals per group. Furthermore, OZR ($n = 10$) and LZR ($n = 10$) were also ramdomised into four experimental groups and subjected to a 4-day study with five animals per group. Treatment groups were as follows: 2 control groups (obese and lean) treated with vehicle (50% saline solution and 50% DMSO, i.p, q.d) and 2 treatment groups (obese and lean) treated with the AMPK activator **A769662** (20 mg·kg^{-1} i.p, q.d for mice and 10 mg·kg^{-1} i.p, q.d for Zucker rats). Two hours after last treatment administration, blood samples were taken for glucose and lactate levels determination by commercial strips with Accutrend Plus measurer. Animals were killed and the kidneys were quickly removed and placed in cold PSS. Biological samples (arteries and cortex samples) were further randomly separated for the various experimental procedures in groups from a number of animals *n* of at least five per group.

2.3 | Dissection and mounting of microvessels

Renal interlobar arteries, second- to third-order branches of the major renal artery, were isolated from the kidney of Zucker rats and *ob/ob* mice and carefully dissected by removing the surrounding connective and fatty tissue. For some experiments, mesenteric resistance arteries of Zucker rats were also dissected. Small samples of both renal arteries and cortex from rats and samples of renal cortex and myocardium from mice were also taken for ROS measurements, as described earlier (Muñoz et al., 2017, 2020). Arterial segments were mounted in microvascular myographs (Danish Myotechnology, Denmark) and equilibrated for 30 min in PSS maintained at 37°C and continuously bubbled with 5% CO_2 in O_2 to maintain pH at 7. The relationship between passive wall tension and internal circumference was determined for each individual artery and from this, the internal circumference L_{100} corresponding to a transmural pressure of 100 mm Hg for a

relaxed vessel in situ was calculated. The arteries were set to an internal diameter I_1 equal to 0.9 times I100 ($L_1 = 0.9 \times L100$), because force development in intrarenal arteries is close to maximal at this internal lumen diameter (Muñoz et al., 2015).

2.4 | Experimental procedures for the functional experiments

At the beginning of each experiment, arteries were stimulated twice with 120 mM K^+ (KPSS) in order to test vessel viability. Integrity of the vascular endothelium was assessed by the relaxations induced by the endothelial agonist **acetylcholine** (ACh). Renal arteries from lean animals with a percentage of ACh-induced relaxation lower than 50% of the **phenylephrine**-induced precontraction, and arteries from obese rats with ACh-induced relaxation lower than 30% were discarded (Muñoz et al., 2015). Cumulative concentration–responses curves to ACh and to the β-adrenoceptor agonist **isoprenaline** were performed on interlobar arteries from LZR and OZR rats or lean and *ob/ob* mice precontracted with **phenylephrine** (0.1–0.5 μM). The relaxation evoked by AMPK activation was assessed with 3 μM and 10 μM of the AMPK selective activator **A769662** in intrarenal arteries and also in mesenteric arteries of LZR and OZR. Arteries were exposed to different drugs until the response reached a plateau. In the case of ACh and **isoprenaline**, quick acting drugs, times of exposure averaged 3 min, whereas for the slow acting AMPK activator A769662, time of exposure averaged 10 min (Rodríguez et al., 2020). To assess the relationship between AMPK and the endothelial PI3K-Akt-eNOS pathway, functional responses to isoprenaline and A769662 were obtained in the absence and presence of the NOS inhibitor, L-NOARG (N^{ω}-nitro- L-arginine; 100 μM) or the PI3K inhibitor (**LY-294002**, 3 μM). Some experiments were performed in endothelium-denuded renal arteries to compare the effect of A769662 in vascular smooth muscle (VSM) of LZR and OZR. The endothelium was mechanically removed by inserting a human hair in the vessel lumen and guiding it back and forwards several times. The absence of functional endothelium was confirmed by lack of the relaxation to ACh (10 μM).

2.5 | Ex vivo acute treatment of Zucker rats preglomerular arteries with A-769662

In order to evaluate the effects of AMPK activation on renal endothelium-dependent relaxations, relaxations to ACh were assessed before and after incubation for 40 min with A769662 (10 μM) in interlobar arteries from LZR and OZR.

2.6 | Measurement of superoxide production by chemiluminescence

Changes in basal and NADPH-stimulated levels of superoxide ($O_2^{\bullet -}$) were measured by lucigenin chemiluminescence in renal arteries and cortex of Zucker rats and in samples of renal cortex and myocardium of lean and obese mice, as earlier reported (Muñoz et al., 2017, 2018, 2020). Tissue samples were dissected and equilibrated in PSS for 30 min at room temperature and then incubated in the absence (basal) and presence of AMPK selective activator A769662 (30 μM) for 30 min at 37°C. Samples were then transferred to microtiter plate wells containing 5 μM bis-*N*-methylacridinium nitrate (lucigenin) and stimulated with NADPH (100 μM) which was added prior to ROS measurements. Chemiluminescence was measured in a luminometer (BMG Fluostar Optima), and for calculation baseline values were subtracted from the counting values under the different experimental conditions and superoxide production was normalized to dry tissue weight.

2.7 | Measurement of hydrogen peroxide by Amplex Red

Hydrogen peroxide (H_2O_2) production was measured by Amplex Red assay Kit (Thermo Fisher Scientific, Life Technologies SA, Madrid, Spain) in renal arteries and cortex of Zucker rats (Muñoz et al., 2017, 2018, 2020). Samples were equilibrated in HEPES-physiological saline solution (PSS) for 30 min at room temperature and then incubated in the absence (basal) and presence of the AMPK selective activator A769662 (30 μM) for 30 min at 37°C. Samples were then transferred to microtiter plate black wells containing Amplex Red (10 mM final concentration) and HRP (10 $U \cdot ml^{-1}$ final concentration), and some were stimulated with NADPH (100 μM) just prior to determination. Fluorescence was measured in a fluorimeter (BMG Fluostar Optima), using an excitation filter of 544 nm and an emission filter of 590 nm. Background fluorescence was subtracted from the counting values under the different experimental conditions and H_2O_2 production was normalized to dry tissue weight.

2.8 | Western blot analysis

Interlobar arteries from LZR and OZR incubated 30 min with A769662 or vehicle and renal cortex samples from *ob/ob* mice and lean treated with vehicle or A769662 were snap frozen in liquid nitrogen, homogenized and lysed in lysis buffer. Protein lysates (13 μg for renal arteries and 20 μg for cortex samples) were separated in a 6.5% polyacrylamide gel (SDS-PAGE), electrotransferred on a PVDF membrane and probed with the following primary antibodies: pACC Ser^{79} (1:1000; ref 3661, RRID:AB_330337), pAMPKα Thr^{172} (1:1000; ref 2535, RRID:AB_331250), $AMPK\alpha_{1/2}$ (1:1000; ref 2532, RRID:AB_330331), pAkt Ser^{473} (1:500; ref 9271, RRID:AB_329825), **Akt** (1:500; ref 9272, RRID:AB_329827), p-eNOS Ser^{1177} (1:500; ref 9571, RRID:AB_329837), **eNOS** (1:500; ref 32027, RRID:AB_2728756) and **TNF-α** (1:1000; ref 11948, RRID:AB_2687962) from Cell Signalling Technology (RRID:SCR_004431) (Leiden, The

Netherlands); **NADPH oxidase 4** (1:500; ref ab154244) from Abcam (RRID:SCR_012931) (Cambridge, UK); p-IKKα/β (Ser 180/Ser 181) (1:1000; ref. 23470), **IKKβ** (P-20) (1:1000; ref 34673), NF-κB p65 (C-20) (1:1000; ref 372) from Santa Cruz Biotechnology (RRID: SCR_008987); β-actin (1:5000; ref A5316) from Sigma (RRID: SCR_008988)(St. Louis, MO, USA) (Contreras et al., 2017; Martinez-Sanchez et al., 2017). Bound primary antibody was detected with HRP conjugated secondary antibodies and blots were visualized using enhanced chemiluminescence and quantified by densitometry with ImageJ (RRID:SCR_003070) free software. Protein expression levels were normalized to β-actin, and then the media ratio of the control group (lean vs. obese or vehicle-treated vs. A769662-treated) was taken as 100%. Original scan images are available in the supporting information.

2.9 | Data presentation and statistical analysis

The data and statistical analysis comply with the recommendations of the *British Journal of Pharmacology* on experimental design and analysis in pharmacology (Curtis et al., 2018). For the functional experiments, results are expressed as either Nm of force, Nm^{-1} of tension or as a percent of the response to **phenylephrine** in each artery, as means ± SEM of six to 12 arteries from five to six animals. For the measurement of $O_2^{\bullet -}$ or H_2O_2 production, results are expressed in counts per minute (cpm) per mg of tissue and relative fluorescence units (RFU) per mg of tissue in arterial segments and cortex samples, respectively, as means ± SEM of five to 12 arteries/cortex samples from of $n = 5–10$ animals. For western blot analysis results are expressed as means ± SEM of five to 11 animals. When two samples from the same animal were used, the average value was taken for the statistical analysis and n was the number of animals.

In order to not to employ an unnecessary amount of animals and to get evidence for an effect of reasonable size in experimental groups, the number of experiments was selected during experimental design and based on considerations of the 3R principles. The experience of our previous investigations was also taken into account, and the minimum number of animals in each group was 5, except for one set of experiments in Figure S2 where there are some groups with $n = 4$, and therefore, comparisons between groups were not undertaken. The group size is the number of independent values, and statistical analysis was undertaken using these independent values. Outliers were included in data analysis and presentation. Data analysis was performed blinded.

Statistically significant differences between means of two groups were analysed by using paired or unpaired Student's *t*-test where appropriate, or one-way ANOVA followed by Bonferroni's post hoc test for comparisons involving more than two groups, when F was significant. P values <0.05 were considered significant. Outliers were included in the analysis. All statistical analysis was calculated using GraphPad Prism 8 (GraphPad Software, RRID: SCR_002798).

2.10 | Materials

A769662 and LY-294002 were supplied by Tocris Cookson (Bristol, UK). Sigma-Aldrich Merck Life Science S.L.U (Madrid, Spain) supplied L-NOARG, isoprenaline and phenylephrine.

2.11 | Nomenclature of targets and ligands

Key protein targets and ligands in this article are hyperlinked to corresponding entries in the IUPHAR/BPS Guide to PHARMACOLOGY (http://www.guidetopharmacology.org) and are permanently archived in the Concise Guide to PHARMACOLOGY 2019/20 (Alexander, Fabbro et al., 2019; Alexander, Kelly, et al., 2019; Alexander, Mathie et al., 2019).

3 | RESULTS

3.1 | General parameters

Metabolic parameters of lean and obese rats used in the study are shown in Table 1. OZR exhibited a marked increase in body and kidney weight, moderate hyperglycaemia, hyperinsulinaemia, hypercholesterolemia and hypertriglyceridemia compared with corresponding values in the LZR. The normalized internal lumen diameters, I_1, were not significantly different in second- to third-order branches renal interlobar arteries from LZR (329 ± 10 μm, $n = 28$ arteries from 15 rats) compared with those of OZR (322 ± 11 μm, $n = 27$ arteries from 15 rats). The relaxations to ACh in the OZR group (51% ± 4, $n = 25$ arteries from 15 rats) were significantly impaired compared with those in the LZR group (67% ± 3, $n = 28$ arteries from 15 rats).

Metabolic parameters of lean and *ob/ob* mice are shown in Table 2. Kidney and body weight and daily food intake were significantly higher in *ob/ob* mice than in lean controls. Plasma glucose levels were elevated in obese mice, whereas plasma triglycerides and cholesterol have been reported to be also higher in this strain, compared with lean controls (Cool et al., 2006). Normalized internal lumen diameters, I_1, were not significantly different in first- to second-order

TABLE 1 Metabolic parameters of LZR and OZR

	LZR	*n*	OZR	*N*
Body weight (g)	399 ± 5	33	482 ± 6*	35
Kidney weight (g)	2.26 ± 0.07	8	2.55 ± 0.16*	8
Glucose (mg ml^{-1})	1.14 ± 0.11	16	1.87 ± 0.22*	19
Insulin (pg ml^{-1})	13 ± 1.7	7	38 ± 3.4	8
Cholesterol (mg ml^{-1})	0.92 ± 0.03	16	1.89 ± 0.10*	18
Triglycerides (mg ml^{-1})	0.94 ± 0.10	16	3.20 ± 0.26*	18

Note: LZR, lean Zucker rats; OZR obese Zucker rats. Data are means ± SEM of the number *n* of animals.

*$P < 0.05$, significantly different from LZR; unpaired Student's *t*-test.

TABLE 2 Metabolic parameters of lean and ob/ob vehicle or A769662-treated mice

	Lean vehicle	Lean-A769662	ob/ob vehicle	ob/ob-A769662
Body weight (g)	25.6 ± 0.8	27.10 ± 0.5	39 ± 2.9*	37.6 ± 3.1
Daily food intake (g)	2.2 ± 0.13	2.2 ± 0.15	2.9 ± 0.5*	1.1 ± 0.3#
Kidney weight (g)	0.26 ± 0.01	0.24 ± 0.01	0.29 ± 0.01*	0.26 ± 0.03
Glucose (mg ml^{-1})	1.27 ± 0.07	1.34 ± 0.01	3.28 ± 0.64*	1.99± 0.11#
Lactate (mM)	4.08 ± 0.24	4.23 ± 0.72	5.36 ± 0.32*	2.88 ±0.29#

Note: Data are means ± SEM of $n = 5–7$ animals in each group.
*$P < 0.05$, significantly different from lean vehicle mice, #$P < 0.05$ significantly different from ob/ob vehicle mice; one-way ANOVA followed by Bonferroni test.

branches renal interlobar arteries from *ob/ob* mice (278 ± 30 μm, 10 arteries from $n = 5$ mice) compared with those in their lean littermates (247 ± 19 μm, 8 arteries from $n = 6$ mice).

3.2 | Impaired endothelial Akt/eNOS/NO vasodilator pathway in preglomerular renal arteries in obesity

Endothelial function was evaluated by the relaxations to ACh and to the non-selective β_1 and β_2-adrenoceptor agonist isoprenaline in renal arteries from LZR and OZR. Activation of β-adrenoceptors, mainly located on vascular smooth muscle (VSM), produces vasodilation mediated by AMPc, although endothelial cells also express β-adrenoceptors whose activation leads to NO production and vasorelaxation via the PI3K/Akt/eNOS pathway (Banquet et al., 2011; Chruscinski et al., 2001; Ferro et al., 2004). Endothelium-dependent relaxations to both ACh and isoprenaline were significantly reduced in obese compared with lean rats (Figure 1a,b; Table 3). Mechanical endothelium removal and inhibition of eNOS (Figure 1c,d) or PI3K blockade (Figure 1g,h; Table 3) markedly reduced the relaxations induced by isoprenaline in intrarenal arteries of LZR but not in those of OZR, thus indicating that the endothelial Akt/eNOS/NO pathway in preglomerular arteries is impaired in obese rats. Western blot analysis confirmed that basal activity of this endothelial pathway was markedly reduced in arteries from obese rats because both levels of p-eNOS and p-Akt (Figure 1e,i) and expression of eNOS and Akt (Figure 1f,j) were significantly lower in OZR renal preglomerular arteries than in LZR arteries.

3.3 | Impaired AMPK activity and renal and systemic AMPK-induced vasorelaxation in obesity

Relaxations elicited by the selective AMPK activator A769662 (10 and 30 μM) were significantly reduced in renal interlobar arteries and also mesenteric arteries of OZR compared with LZR (Figure 2a–d). Impaired relaxations to A769662 were associated with reduced AMPK activity in renal arteries of OZR, compared with values from LZR. Thus, Western blot analysis of artery homogenates revealed a decreased AMPKα phosphorylation (Figure 2e) and expression (Figure 2f) of in arteries from OZR. In keeping with those data, p-ACC protein levels were also reduced in OZR renal arteries (Figure 2g).

The involvement of the endothelial PI3K/eNOS/NO pathway in the impaired relaxations elicited by AMPK activation in preglomerular arteries of obese rats was further assessed. Mechanical endothelial cell removal and pharmacological blockade of NOS (by L-NOARG) or PI3K (by LY-294002) significantly reduced the relaxations to A769662 in arteries of LZR (Figure 3a,d,g). In contrast, A769662-induced relaxations after removal of endothelium or inhibition of NOS or PI3K were unchanged or even enhanced in preglomerular arteries of OZR, compared with controls (Figure 3b,e,h). The magnitude of these relaxations was not different from that in LZR arteries after removal of endothelium or blockade of NOS or PI3K (Figure 3c,f,i). Overall, these data indicate that endothelium-dependent vasodilation induced by AMPK activation is altered due to impaired endothelial/PI3K/eNOS pathway in obese rats, whereas endothelium-independent AMPK VSM-mediated relaxations in preglomerular arteries are preserved in obese rats.

3.4 | Acute in vitro AMPK treatment improves metabolic activity and restores endothelial function of intrarenal arteries in obesity

AMPK dysregulation has been identified as a major risk for development of CKD in obesity, metabolic syndrome and diabetes (De Vries et al., 2014; Decleves et al., 2011; Dugan et al., 2013) and specific AMPK activation in the kidney has been proposed as a potential target to improve renal function (Salatto et al., 2017). Therefore, in order to investigate whether acute treatment with AMPK activator is beneficial for endothelial function in obesity, renal arteries from LZR and OZR were incubated ex vivo with A769662 for 40 minutes before a second concentration–response curve for the endothelial agonist ACh was performed. As shown in Figure 4, acute in vitro treatment with the AMPK activator A769662 did not significantly change relaxations to ACh in control rats (Figure 4a) but increased ACh-induced vasodilation in arteries from OZR (Figure 4b).

Western blot analysis demonstrated that ex vivo incubation of renal preglomerular arteries with A769662 increased phosphorylation of the AMPK downstream target ACC in LZR (Figure 4c) and also in OZR (Figure 4d). Moreover, p-eNOS and eNOS protein levels were markedly enhanced in arteries from lean rats after treatment with

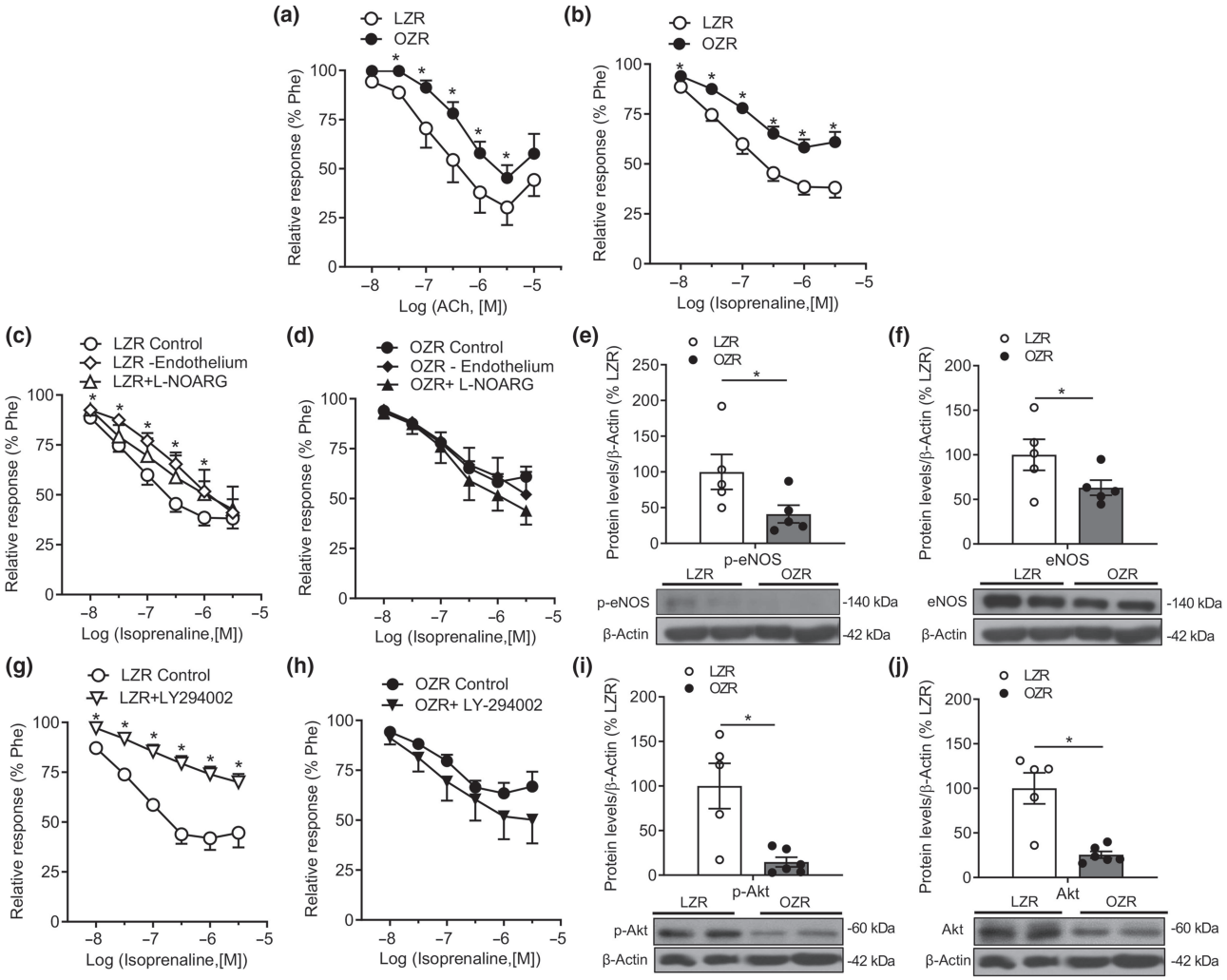

FIGURE 1 PI3K/Akt/eNOS/NO vasodilator pathway in endothelium is impaired in renal preglomerular arteries of OZR along with reduced activity and down-regulation of Akt and eNOS. (a,b) Relaxations to ACh (a) and isoprenaline (b) in renal interlobar arteries from LZR and OZR. (c,d, g,h) Vasodilator responses to isoprenaline in renal arteries of LZR and OZR under different experimental conditions: in endothelium-denuded arteries, in the presence of the NOS synthase inhibitor L-NOARG (100 μM) (c,d) and in the presence of inhibitor of PI3K, LY-294002 (3 μM) (g,h). Results are expressed as percentage of the increases in tension induced by phenylephrine (Phe). Data are shown as the mean ± SEM of six to 10 arteries from $n = 5$ LZR and $n = 5$ OZR. *$P < 0.05$, significantly different from LZR or OZR control responses in the absence of inhibitors; Student's *t*-test for paired observations. (e,f,i,j) Western blot analysis for p-eNOS (e), eNOS (f), p-Akt (i), Akt (j) in renal arteries from LZR and OZR. Results were normalized to β-actin content in samples. Data represent mean ± SEM values of $n = 5$ LZR and 5 OZR rats (e,f) and $n = 5$ LZR and 6 OZR rats (i,j). *$P < 0.05$, significantly different from LZR; Student's *t*-test for unpaired observations

TABLE 3 Relaxant effects of isoprenaline in renal interlobar arteries from LZR and OZR before and after mechanical endothelium removal or inhibition of eNOS or PI3K blockade

	LZR					OZR				
	pEC_{50}	E_{max}	*n*	I_1	KPSS	pEC_{50}	E_{max}	*n*	I_1	KPSS
Isoprenaline	6.40 ± 0.14	61.4 ± 3.9	15	311 ± 15	1.55 ± 0.25	5.28 ± 0.33*	41.7 ± 4*	12	321 ± 18	0.70 ± 0.15
− Endothelium	5.89 ± 0.03#	48.3 ± 5.1#	8	293 ± 35	0.77 ± 0.21	5.51 ± 0.11*	39.1 ± 9.5	6	283 ± 18	0.43 ± 0.10
+ L-NOARG	5.96 ± 0.1#	49.6 ± 12.1	7	330 ± 20	1.5 ± 0.5	5.89 ± 0.1	48.3 ± 7.7	6	295 ± 44	0.67 ± 0.16
Isoprenaline	6.30 ± 0.22	58.1 ± 5.9	6	315 ± 31	1.38 ± 0.42	4.88 ± 0.47*	36.5 ± 5*	6	330 ± 34	0.95 ± 0.3
+ LY294002	4.53 ± 0.25#	26.1 ± 3.9#	6	394 ± 45	2.10 ± 0.51	5.76 ± 0.16	48.1 ± 11	6	344 ± 35	1.42 ± 0.4

Note: Values represent mean ± SEM of the number *n* of individual arteries from five LZR and five OZR (one or two per animal). pEC50 is $-\log EC_{50}$, EC_{50} being the agonist concentration giving half-maximal relaxation; E_{max} = maximal relaxation (% Phe); I_1 = internal diameter (μm); KPSS (Nm^{-1}).
*$P < 0.05$, significantly different from LZR, #$P < 0.05$, significantly different from control before treatment; unpaired Student's *t*-test.

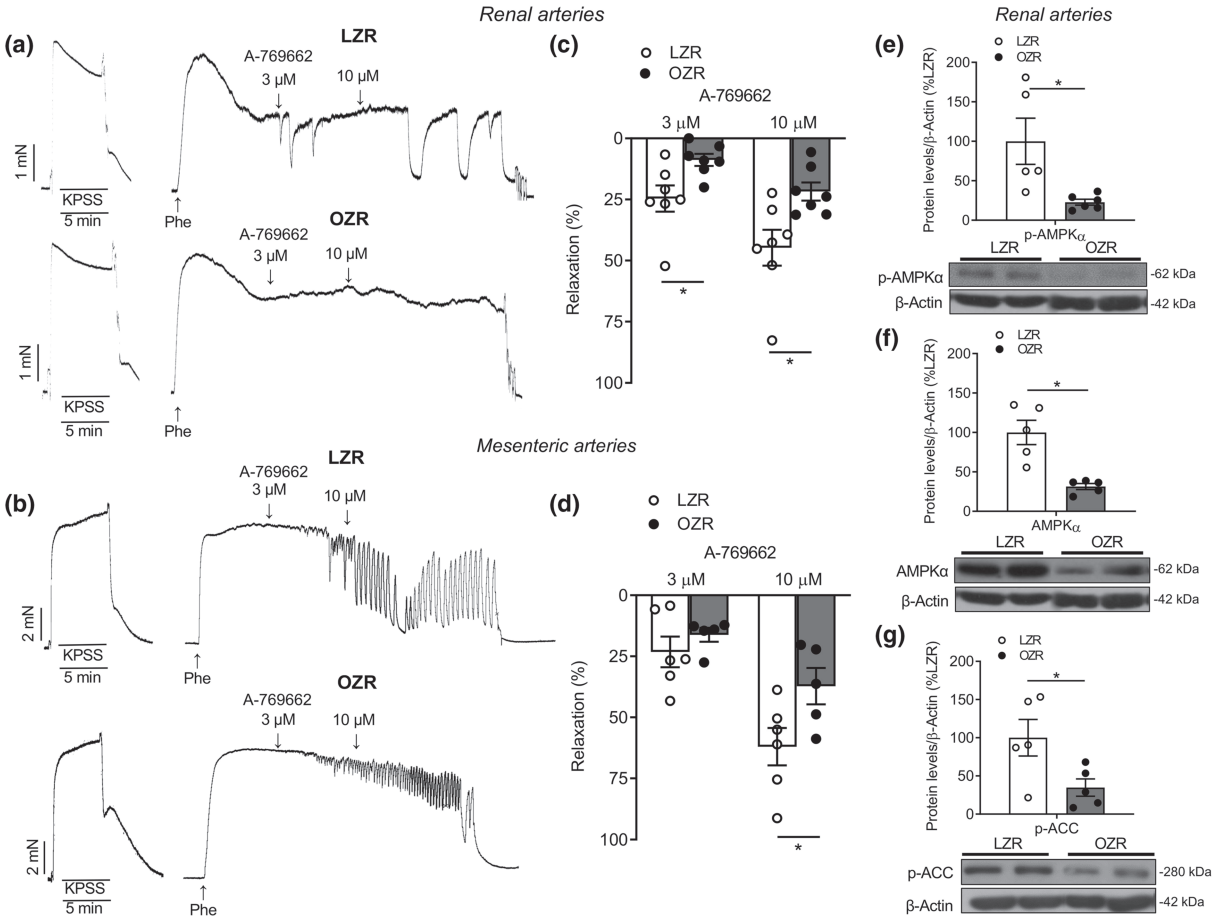

FIGURE 2 Relaxations induced by the AMPK activator A769662 are reduced in small renal and mesenteric arteries in obesity, which is associated with impaired AMPK activity and expression. (a,b) Original recordings showing A769662-induced relaxations in renal (a) and mesenteric (b) arteries from LZR and OZR and (c,d) average vasodilator effect of A769662 (3 and 10 μM). Results are expressed as percentage of the increases in tension induced by phenylephrine (Phe). Data are shown as the mean ± SEM of five to 10 arteries from $n = 5$ LZR and $n = 5$ OZR. *$P < 0.05$, significantly different from LZR or OZR control responses; Student's t-test for paired observations. (e-g) Western blots analysis for p-AMPKα (e), AMPKα (f) y p-ACC (g) protein levels in samples of renal arteries from LZR and OZR. Results were quantified by densitometry and presented as a ratio of density of the protein band to that of β-actin from the sample. Data are shown as the mean ± SEM of $n = 5$ LZR and $n = 6$ OZR (e), $n = 5$ LZR and $n = 5$ OZR (f,g). *$P < 0.05$, significantly different from LZR; Student's t-test for unpaired observations

A769662 (Figure 4e,g), thus confirming the involvement of the endothelial PI3K/eNOS/NO pathway in AMPK-induced dilatation of renal arteries. In arteries from OZR, acute treatment with A769662 increased protein levels of eNOS but not p-eNOS (Figure 4f,h).

In order to further investigate whether AMPK activation may be beneficial for renal endothelial function in obesity, we tested the in vivo effects of A769662 administration in genetically obese mice. Endothelial function of preglomerular arteries and β-adrenoceptor and AMPK-mediated vasodilation were assessed in interlobar arteries from *ob/ob* and lean mice. As found for arteries of OZR, endothelium-dependent ACh and isoprenaline vasodilator pathways as well as AMPK-mediated vasorelaxation were impaired in arteries from *ob/ob* mice, compared with those in lean mice (Figure 5a–c) (Table 4). Interestingly, in contrast to the impaired endothelial relaxations in preglomerular arteries, there was a pronounced increase in basal p-eNOS and eNOS levels (Figure S1c,d) in cortical samples from *ob/ob* mice compared with controls, suggesting an up-regulation of the endothelial eNOS/NO pathway in renal cortex of obese mice. Western blot analysis also revealed that basal phosphorylation of AMPKα (Figure S1a) and of its downstream target ACC (Figure S1b) were significantly higher in renal cortex of obese compared with lean mice. These data thus show endothelial dysfunction and AMPK dysregulation in renal preglomerular resistance arteries of *ob/ob* mice, whereas there was up-regulation of eNOS and AMPK activities in renal cortex of obese animals.

3.5 | In vivo AMPK treatment restores endothelial function in preglomerular arteries and improves metabolic and AMPK activity in renal cortex of *ob/ob* mice

Metabolic parameters of lean and *ob/ob* mice treated with vehicle or A769662 are shown in Table 2. A769662 administration improved

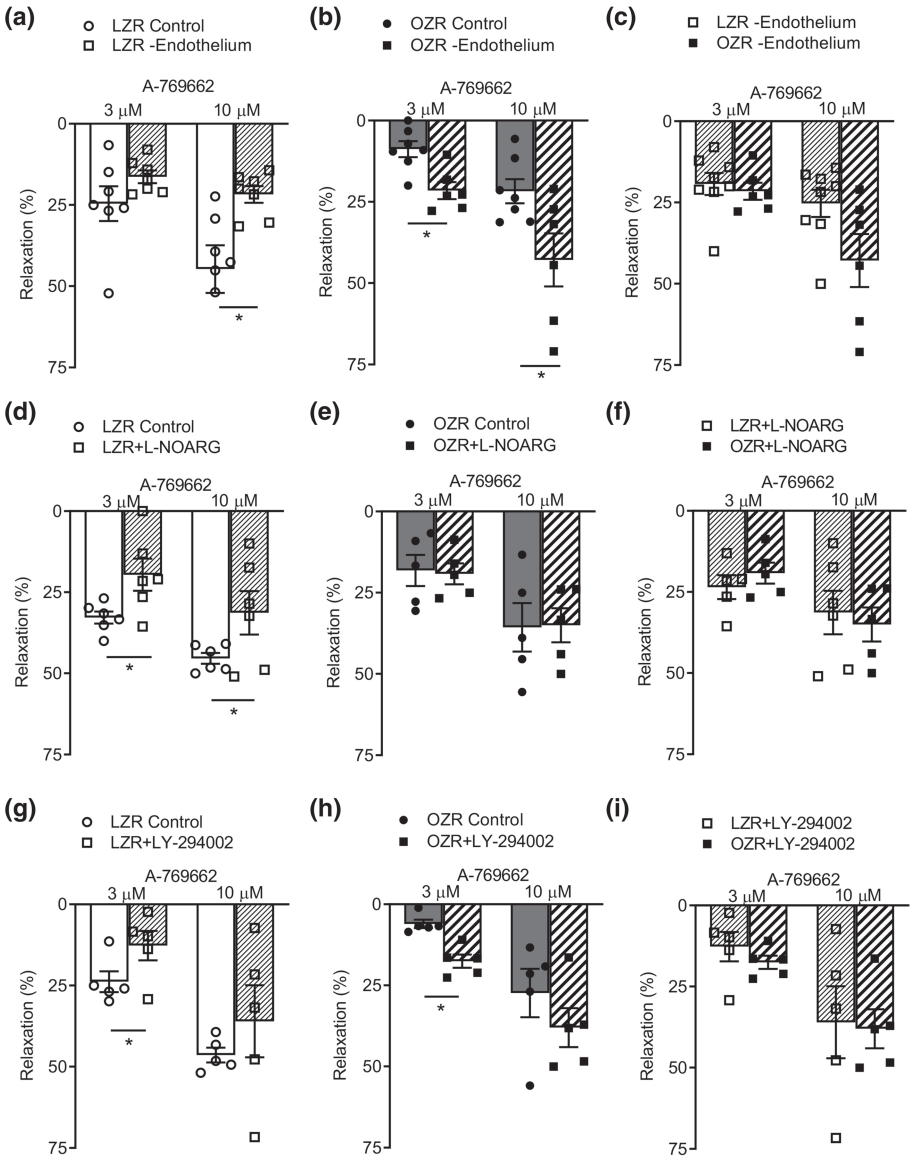

FIGURE 3 The AMPK/PI3K/eNOS pathway in renal endothelium is impaired in obesity. (a-b) Average vasodilator effect of 3 and 10 μM of A769662 in endothelium-intact and endothelium-denuded renal arteries from LZR (a) and OZR (b). Effect of the NOS synthase inhibitor L-NOARG (100 μM) and PI3K inhibitor (LY-294002, 3 μM) on A769662-induced vasodilation in renal arteries from LZR (d,g) and OZR (e,h) before and after treatment with inhibitors. Comparison of vasodilator response to A769662 after removal of endothelium or treatment with both inhibitors in LZR and OZR (c,f,i). Results are expressed as percentage of the increases in tension induced by phenylephrine (Phe). Data are shown as the mean ± SEM of five to seven arteries from $n = 6$ LZR and $n = 6$ OZR. *$P < 0.05$, significantly different from LZR or OZR control responses in the absence of inhibitors; Student's *t*-test for paired observations

plasma glucose and lactate levels, reduced kidney weight and induced a trend to reduce body weight and daily food intake in *ob/ob* mice (Table 2; Figure S2).

After a 4-day in vivo treatment with A769662 or vehicle, endothelial/vascular function of renal interlobar arteries from *ob/ob* mice and lean controls was assessed in arteries mounted in parallel in microvascular myographs. As shown in Figure 5d,e and Table 4, vasodilator responses to ACh or to the β-adrenoceptor agonist isoprenaline in arteries from lean mice were similar in vehicle- and A769662-treated groups. However, A769662-treatment significantly increased ACh- (Figure 5d) and isoprenaline- (Figure 5e) induced vasorelaxation in renal arteries of *ob/ob* mice compared with those of vehicle-treated obese mice. Comparison of ACh and isoprenaline relaxations in the *ob/ob*-treated group to those in vehicle-treated lean group, confirmed that in vivo treatment with the AMPK activator A769662 reversed the loss of both isoprenaline-induced relaxations and ACh endothelium-dependent vasodilation in *ob/ob* mice (Figures 5d and e). On the other hand, A769662 treatment enhanced eNOS phosphorylation at Ser1177 in renal cortex from lean (Figure 5f) but not obese mice (Figure 5g) wherein both eNOS and p-eNOS Ser^{1177} were already up-regulated (Figure S1c,d). In vivo activation of AMPK improved metabolic activity in renal cortex of both lean and *ob/ob* mice compared with the vehicle group, as shown by the increased phosphorylation of AMPKα (Figure 5h,i).

3.6 | Anti-inflammatory role of in vivo AMPK activation by suppressing NF-κB signalling in kidney of *ob/ob* mice

Excessive accumulation of fatty acids in skeletal muscle and other organs in obesity and metabolic syndrome leads to activation of the NF-κB signalling pathway that increases circulating cytokines and produces systemic inflammation. AMPK activation has important anti-

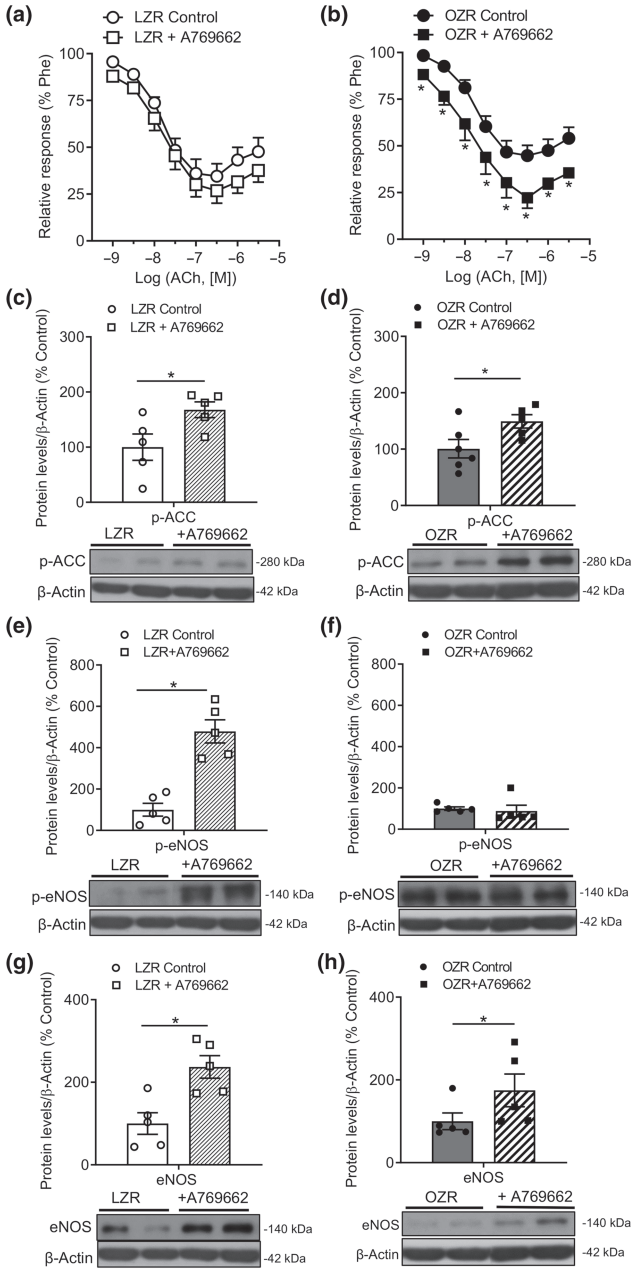

FIGURE 4 Ex vivo acute treatment with A769662 ameliorates endothelial dysfunction and increases eNOS protein levels in OZR preglomerular arteries. (a,b) In vitro effect of the AMPK activator A769662 on the relaxations to ACh of LZR (a) and OZR (b) renal interlobar arteries. Results are expressed as percentage of the precontraction induced by phenylephrine (Phe). Data are shown as the mean ± SEM of six to 10 arteries from $n = 5$ LZR and $n = 5$ OZR. *$P < 0.05$, significantly different from LZR or OZR without treatment with A769662; Student's *t*-test for paired observations. (c,h) Western blot analysis for p-ACC, p-eNOS and eNOS protein levels in samples of renal arteries from LZR (c,e,g) and OZR (d,f,h) with or without ex vivo treatment with A769662 (10 μM). Results were normalized to β-actin content in samples. Data represent mean ± SEM values of $n = 5$ LZR and $n = 5$–6 OZR. *$P < 0.05$, significantly different from LZR or OZR without incubation with A769662; Student's *t*-test for unpaired observations

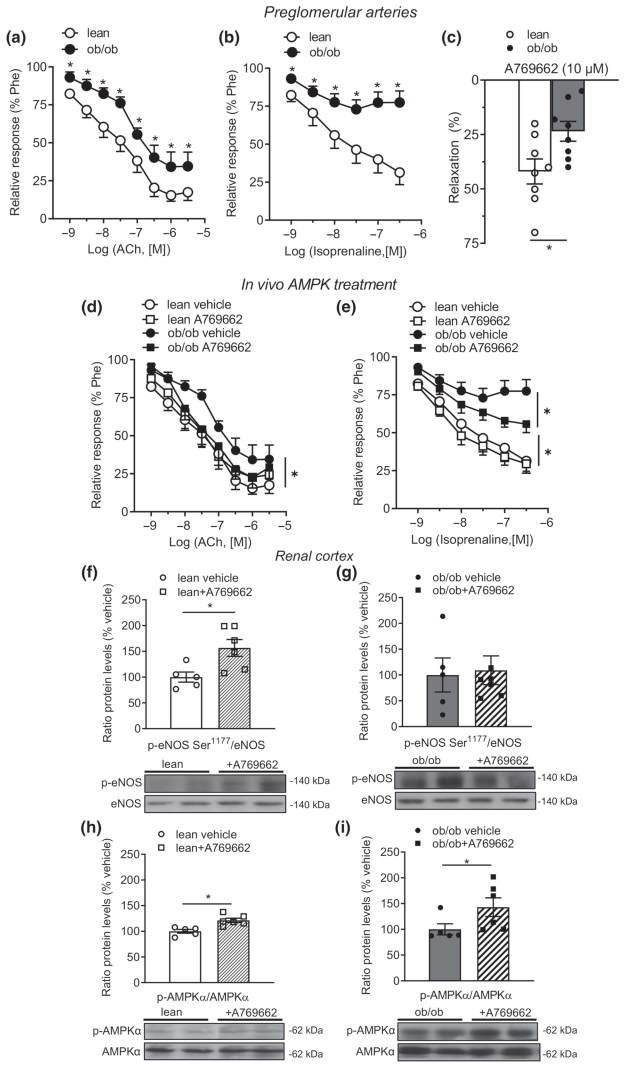

FIGURE 5 In vivo AMPK activation with A769662 improves relaxations to ACh and isoprenaline in preglomerular arteries of *ob/ob* mice. Relaxations to ACh (a), isoprenaline (b) and A769662 (10 μM) (c) in renal interlobar arteries from lean and *ob/ob* mice. Results are expressed as percentage of the precontraction induced by phenylephrine (Phe). (d-e) Comparison of the relaxations to isoprenaline and ACh in preglomerular arteries of lean (d) and *ob/ob* mice (e) treated with vehicle versus mice treated with A769662. In vivo treatment with the AMPK activator restored the loss of endothelium-dependent vasodilation of obese mice because isoprenaline-induced relaxations (e) and vasodilation to ACh (d) were larger when compared with relaxations of *ob/ob* mice treated with vehicle. Data are shown as the mean ± SEM of seven to 10 arteries of $n = 5$ lean mice and $n = 7$ *ob/ob* mice. *$P < 0.05$, significantly different from lean mice (a–c) or vehicle-treated lean or *ob/ob* mice (d,e); Student's *t*-test for unpaired (a–c) or (d, e) one-way ANOVA followed by Bonferroni post test. (f–i) Western blot analysis for ratio p-eNOS/eNOS in samples of renal cortex from lean (f) *ob/ob* mice (g) with or without A769662 treatment, as well as p-AMPKα/AMPKα ratio in lean (h) *ob/ob* mice (i). Results are expressed as percentage vehicle-treated lean or *ob/ob* mice. Data represent mean ± SEM values of $n = 5$ and $n = 6$ (f,h,i), $n = 5$ and $n = 6$ (g) vehicle-treated and A769662-treated mice, respectively. *$P < 0.05$, significantly different from vehicle-treated lean or *ob/ob* mice; Student's *t*-test for unpaired observations. Outliers were included in analysis (g)

TABLE 4 Relaxant effects of ACh and isoprenaline in renal interlobar arteries from lean and ob/ob mice compared with A769662-treated mice

Lean vehicle						Lean-A769662				
	pEC_{50}	E_{max}	*n*	I_1	KPSS	pEC_{50}	E_{max}	*n*	I_1	KPSS
ACh	7.54 ± 0.07	84.6 ± 3.9	7	236 ± 18	0.67 ± 0.17	7.34 ± 0.09	77.3 ± 6.5	10	252 ± 27	0.65 ± 0.15
Isoprenaline	7.54 ± 0.08	68.6 ± 8.0	7	249 ± 22	0.67 ± 0.17	7.79 ± 0.11	70.5 ± 4.9	8	259 ± 29	0.65 ± 0.15
***ob/ob* vehicle**						**ob/ob-A769662**				
	pEC_{50}	E_{max}	*n*	I_1	KPSS	pEC_{50}	E_{max}	*n*	I_1	KPSS
ACh	6.60 ± 0.1$^{\#}$	65.8 ± 9.7$^{\#}$	7	292 ± 36	0.5 ± 0.19	7.15 ± 0.1*	77.6 ± 6.7	7	234 ± 25	0.58 ± 0.14
Isoprenaline	—	22.6 ± 6.9$^{\#}$	7	281 ± 31	0.5 ± 0.19	6.4 ± 0.25	44.3 ± 5.6*	8	234 ± 25	0.58 ± 0.14

Values represent mean ± SEM of 7–10 individual arteries of five lean and five ob/ob mice (1–2 per animal). pEC50 is −logEC50, EC_{50} being the agonist concentration giving half-maximal relaxation; E_{max} = maximal relaxation (% Phe); I_1 = internal diameter (μm); KPSS (Nm^{-1}).
*$P < 0.05$, significantly different from ob/ob vehicle mice; $^{\#}P < 0.05$, significantly different from lean vehicle mice; unpaired Student's *t*-test.

inflammatory effects by suppressing the NF-κB axis (Green, Macrae, et al., 2011; Green, Pedersen, et al., 2011). In order to assess the effect of in vivo treatment with A769662 on the kidney inflammatory response of genetically obese mice, we measured p-IKK, IKK, NF-κB and TNF-α protein levels. Western blot analysis showed that protein levels of p-IKK and TNF-α were significantly increased in renal cortex of *ob/ob* mice compared with controls (Figure 6a,g), but not those of IKK or NF-κB protein (Figure 6c,e). In vivo treatment with A769662 produced a significant reduction of p-IKK (Figure 6b), IKK (Figure 6d), NF-κB (Figure 6f) and TNF-α (Figure 6h) protein expression in renal cortex of *ob/ob* mice when compared with *ob/ob* mice treated with vehicle. These data suggest that in vivo treatment with A769662 suppresses renal inflammation in obese mice.

3.7 | In vivo treatment with A769662 restores impaired kidney NADPH-derived ROS production in renal cortex of *ob/ob* mice

To investigate the antioxidant effects of AMPK activation in the kidney, ROS levels were assessed in renal cortex samples of lean and genetically obese mice after in vivo administration of A769662. Interestingly, $O_2^{\bullet-}$ levels measured by lucigenin chemiluminescence after stimulation with NADPH, were significantly reduced in renal cortex from *ob/ob* mice, compared with lean controls, as shown in Figure 7a. In vivo treatment with A769662 augmented NADPH-stimulated $O_2^{\bullet-}$ levels in cortical samples of *ob/ob* mice (Figure 7b), whereas reduced NADPH-stimulated $O_2^{\bullet-}$ levels in lean mice, compared with those of vehicle-treated lean mice (Figure S3a). These data indicate that in vivo AMPK activation restores the decreased renal cortex levels of ROS in obese to levels similar to those in lean control mice. Furthermore, western blot analysis showed that protein content of Nox4 was significantly reduced in renal cortex from *ob/ob* compared with lean mice (Figure 7c). In vivo treatment with A769662 further significantly reduced Nox4 protein levels in renal cortex from both *ob/ob* mice (Figure 7d), and also those in lean controls (Figure S3b).

On the other hand, NADPH-derived ROS production was measured in myocardium samples of lean and *ob/ob* mice in order to compare the effect of in vivo AMPK activation on heart to the effect on kidney samples. $O_2^{\bullet-}$ levels detected by chemiluminiscence were also significantly reduced in the heart of *ob/ob* mice compared with controls, as shown in Figure 7e. Likewise in renal cortex, in vivo treatment with A769662 reduced NADPH-stimulated $O_2^{\bullet-}$ levels in lean mice (Figure S3c). However, there were no significant differences in NADPH-stimulated $O_2^{\bullet-}$ levels in the myocardium from A769662-treated and vehicle-treated groups of *ob/ob* mice (Figure 7f).

3.8 | Both ex vivo and in vivo AMPK activation with A769662 reduces NADPH-derived ROS production in renal preglomerular arteries from OZR

The antioxidant effects of both in vitro and in vivo AMPK activation on kidney vascular tissues in obesity were investigated in interlobar arteries from LZR and OZR. NADPH-stimulated $O_2^{\bullet-}$ levels were markedly increased in isolated preglomerular arteries of OZR compared with LZR (Figure 8a). In contrast, NADPH-stimulated H_2O_2 generation was significantly decreased in arteries of obese rats compared with lean controls (Figure 8b). Acute in vitro treatment with A769662 induced a powerful suppression of NADPH-stimulated $O_2^{\bullet-}$ in samples of renal arteries from both LZR and OZR as shown in Figure 8a. A769662 also reduced NADPH-stimulated H_2O_2 production in arteries from LZR, and to a lesser extent in OZR, wherein H_2O_2 production was already reduced compared with lean controls (Figure 8b). These data show that the increase in the overall NADPH-derived $O_2^{\bullet-}$ levels contributes to oxidative stress in renal vasculature in obesity, although NADPH-derived H_2O_2 levels are reduced in preglomerular arteries. Interestingly, A769662 acts as an effective vascular antioxidant and can counteract and reduce arterial ROS production in obese rats.

Western blot analysis showed that basal protein levels of Nox4 were significantly lower in renal arteries of OZR compared with LZR

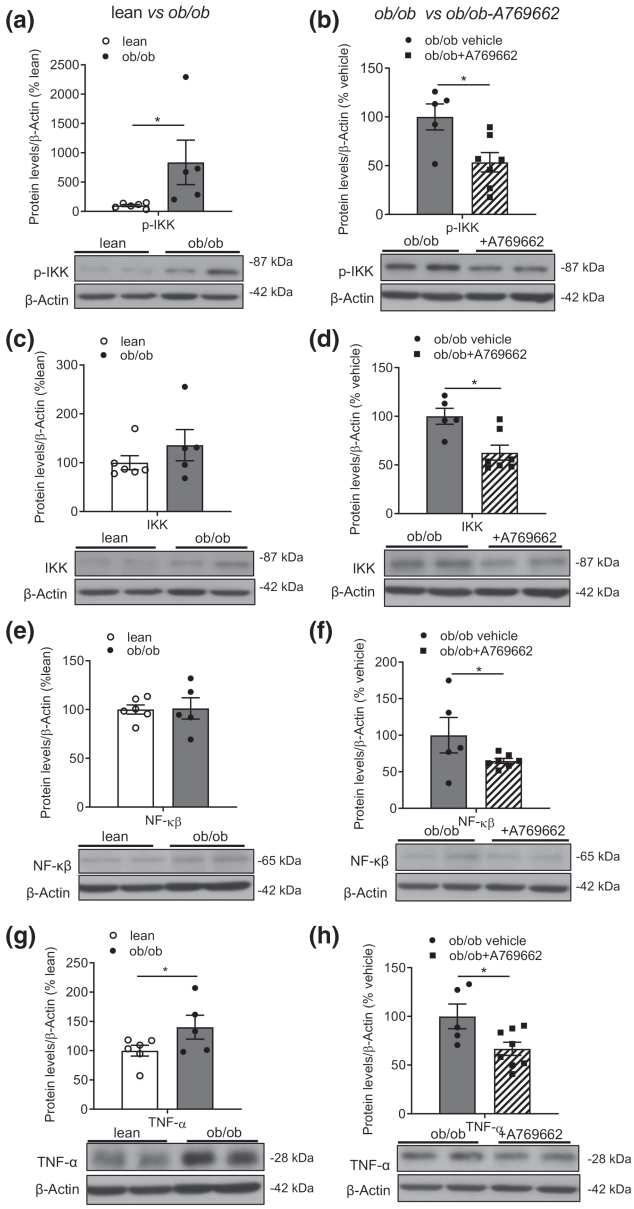

FIGURE 6 In vivo treatment with A769662 reduces inflammatory markers in the kidney of *ob/ob* mice. Western blot analysis for p-IKK (a), IKK (c), NF-κB (e) and TNF-α (g) protein levels in samples of renal cortex from lean and *ob/ob* mice treated with vehicle. Results were normalized to β-actin content in samples and are expressed as percentage of lean mice. Data represent mean ± SEM values of $n = 6$ lean and $n = 5$ of *ob/ob* mice (a,c,e,g). $^{*}P < 0.05$, significantly different from vehicle-treated lean mice; Student's *t*-test for unpaired observations. Western blot analysis for p-IKK (b), IKK (d), NF-κB (f) and TNF-α (h) protein levels in samples of renal cortex from vehicle-treated *ob/ob* mice and A769662-treated *ob/ob* mice. Results were normalized to β-actin content in samples and are expressed as percentage of vehicle-treated *ob/ob* mice. Data represent mean ± SEM values of $n = 5$ and $n = 7$ (b,d,f), and $n = 5$ and $n = 8$ (h) vehicle-treated *ob/ob* mice and A769662-treated *ob/ob* mice, respectively. $^{*}P < 0.05$, significantly different from vehicle-treated *ob/ob* mice; one-way ANOVA followed by Bonferroni post test. Outliers were included in analysis

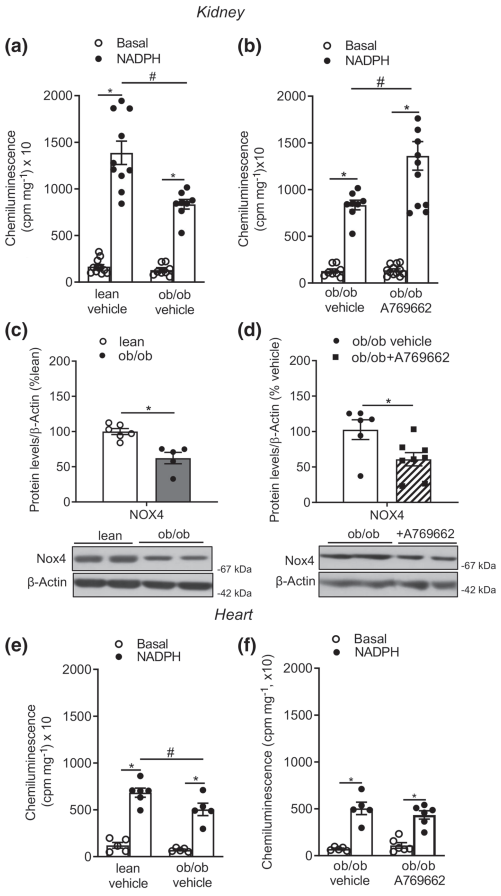

FIGURE 7 In vivo activation of AMPK restores ROS levels in renal cortex of *ob/ob* mice. (a) Basal and NADPH-stimulated $O_2^{\bullet -}$ levels measured by lucigenin-enhanced chemiluminescence in renal cortex samples of vehicle-treated lean and *ob/ob* mice. (b) Comparison between $O_2^{\bullet -}$ levels in renal cortex samples from *ob/ob* mice treated with vehicle or after in vivo administration of A769662. Results are expressed in counts per minute (cpm) per mg of tissue. Bars represent mean ± SEM of $n = 5$ lean and $n = 5$ *ob/ob mice* (one to two cortex samples per animal). $^{*}P < 0.05$, significantly different from basal levels; $^{\#}P < 0.05$, significantly different from vehicle-treated *ob/ob* mice; one-way ANOVA followed by Bonferroni post test. (c,d) Western blots analysis for Nox4 protein levels in renal cortex from lean versus *ob/ob* mice (c) and down-regulation upon chronic in vivo treatment with the AMPK activator A769662 in *ob/ob* (d). Results were quantified by densitometry and presented as a ratio of the density of the Nox4 band to that of β-actin from the sample. Data are shown as the mean ± SEM of $n = 6$ and $n = 5$ lean and *ob/ob* mice, respectively (c), and of $n = 6$ and $n = 8$ vehicle-treated and A769662-treated *ob/ob* mice, respectively (d). $^{*}P < 0.05$, significantly different from lean (c) and *ob/ob* treated with vehicle (d); Student's *t*-test for unpaired observations. (e) Basal and NADPH-stimulated $O_2^{\bullet -}$ levels in myocardial samples of lean and *ob/ob* mice treated with vehicle. (f) Effect of in vivo treatment with A769662 on NADPH-stimulated $O_2^{\bullet -}$ levels in myocardium samples from *ob/ob* measured by lucigenin-enhanced chemiluminescence. Results are expressed in counts per minute (cpm) per mg of tissue. Bars represent mean ± SEM of one to two samples of $n = 5$ lean and $n = 5$ *ob/ob* mice, respectively (e) and $n = 5$ vehicle-treated and $n = 5$ A76962-treated *ob/ob* mice (f). $^{*}P < 0.05$, significantly different from basal levels; $^{\#}P < 0.05$, significantly different from vehicle-treated lean mice; one-way ANOVA followed by Bonferroni post test

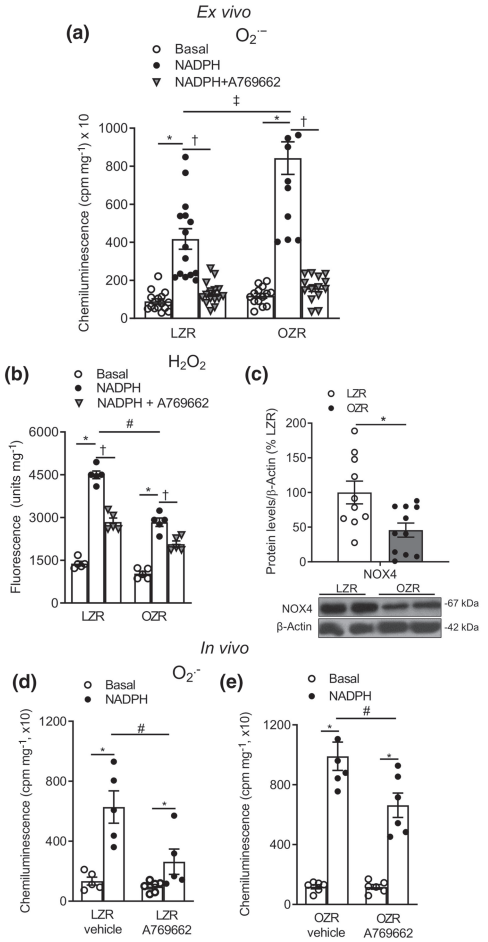

FIGURE 8 Both acute in vitro and in vivo AMPK activation reduce Nox-derived ROS generation in preglomerular arteries of lean and obese Zucker rats. Inhibitory in vitro effect of A769662 (30 μM) on NADPH-stimulated $O_2^{\bullet-}$ (a) and H_2O_2 (b) levels in renal interlobar arteries of LZR and OZR measured by lucigenin-enhanced chemiluminescence and Amplex Red fluorescence, respectively. Results are expressed in counts per minute (cpm) per mg of tissue for chemiluminescence and in relative fluorescence units (RFU) per mg of tissue for fluorescence. Bars represent mean ± SEM of one to two arteries from $n = 7$ LZR and $n = 6$ OZR (a), $n = 5$ LZR and $n = 5$ OZR (b). $^{*}P < 0.05$, significantly different from basal levels, $^{\dagger}P < 0.05$, significantly different from NADPH-stimulated; $^{\#}P < 0.05$, significantly different from LZR; one-way ANOVA followed by Bonferroni post test. (c) Western blots analysis for Nox4 protein levels in renal arteries from LZR versus OZR. Results were quantified by densitometry and presented as a ratio of density of the Nox4 band to that of β-actin from the sample. Data are shown as the mean ± SEM of $n = 10$ LZR and $n = 11$ OZR, respectively. $^{*}P < 0.05$, significantly different from LZR; Student's *t*-test for unpaired observations. (d,e) Comparison between $O_2^{\bullet-}$ levels measured by lucigenin-enhanced chemiluminescence in basal and NADPH-stimulated isolated renal interlobar arteries from LZR (d) and OZR (e) after in vivo treatment with A769662. Results are expressed in counts per minute (cpm) per mg of tissue. Bars represent mean ± SEM of $n = 5$ vehicle-treated and $n = 5$ A76962-treated LZR (d) and $n = 5$ vehicle-treated and $n = 5$ A76962-treated OZR (e). $^{*}P < 0.05$, significantly different from basal levels, $^{\#}P < 0.05$, significantly different from LZR (d) or OZR (e) treated with vehicle; one-way ANOVA followed by Bonferroni post test

(Figure 8c). Moreover, acute treatment with A769662 markedly reduced Nox4 protein levels in renal arteries from both LZR and OZR (Figure S4a,b) thus suggesting that AMPK activation down-regulates Nox4-derived arterial H_2O_2 production from LZR and OZR.

In vivo experiments showed that NADPH-derived ROS were markedly increased in OZR preglomerular arteries compared with those in LZR arteries from vehicle-treated groups (Figure 8d,e). As in the in vitro assay, in vivo administration of A769662 also reduced NADPH-stimulated $O_2^{\bullet-}$ levels in renal preglomerular arteries from LZR (Figure 8d) and OZR (Figure 8e) when compared with groups treated with vehicle. These data indicate that in vivo AMPK activation has vascular antioxidant effects by reducing superoxide levels in renal arteries from obese rats.

4 | DISCUSSION

Obesity is risk factor for the development of CKD, independent of diabetes, hypertension and other co-morbidities and AMPK dysregulation seems to play a key role in inflammation and fibrosis underlying obesity-associated nephropathy (Decleves et al., 2011). Here we have demonstrated that activation of AMPK not only improved metabolic state and decreased inflammation in the kidney of genetically obese animals but also ameliorated endothelial dysfunction and vascular oxidative stress while restoring the redox balance in renal cortex.

AMPK activity is impaired in muscle, liver and kidney under conditions of metabolic stress, such as obesity (Ix & Sharma, 2010; Liu et al., 2005; Motawi et al., 2009). In the kidney, reduced renal AMPK activity was associated with inflammation, increased matrix accumulation, glomerular hypertrophy, tubular injury and albuminuria in high fat diet (HFD)-induced obese mice, and AMPK activation by treatment with AICAR prevented abnormal structural and functional effects of HFD (Decleves et al., 2011; Kume et al., 2007; Szeto et al., 2016). The present findings show that AMPK expression and activity were greatly suppressed in renal arteries of genetically obese rats and were associated with blunted NO-mediated relaxation by the specific AMPK activator A769662, along with reduced phosphorylation of the AMPK downstream target ACC, rate-limiting enzyme for de novo fatty acid synthesis that favours mitochondrial oxidation of fatty acids. While impaired relaxation suggests endothelial dysfunction, decreased ACC activity may be involved in kidney vascular lipotoxicity, as reported for the aortic endothelium of obese OLEFT rats where augmented triglycerides and lipid peroxidation was associated with reduced AMPK activity, reduced NO and endothelial dysfunction (Lee et al., 2005). Therefore, renal dysfunction related to AMPK dysregulation in obesity is not only due to glomerulopathy, fibrosis or lipotoxicity-induced tubular injury (Decleves et al., 2011; Decleves, Sharma & Satriano, 2014; Szeto et al., 2016), but also notably to impairment of the vascular effects of AMPK.

AMPK has recently been involved in the metabolic regulation of kidney blood flow and causes vasodilation of human renal arteries

through both endothelium-dependent and independent mechanisms (Rodríguez et al., 2020). In the present study, decreased relaxant effects of AMPK activation were found in preglomerular arteries associated with endothelial dysfunction and impaired endothelial PI3K/eNOS/NO pathway in obese rats. Thus, relaxations induced by the endothelial agonist ACh and by the β-adrenoceptor agonist isoprenaline were markedly reduced along with diminished basal eNOS and Akt activity and expression in renal arteries of OZR. Endothelial β-adrenoceptors can modulate eNOS and NO-mediated vasodilation through eNOS phosphorylation via different pathways including the PKA/Akt and PI3K/Akt pathways (Banquet et al., 2011; Kou & Michel, 2007), both activated downstream by AMPK. Accordingly, both isoprenaline and AMPK-mediated relaxations were unchanged by endothelial cell removal and resistant to NOS or PI3K blockade in kidney preglomerular arteries of obese rats thus confirming an impaired endothelial PI3K/NOS/NO pathway. Endothelium-mediated AMPK relaxations in renal arteries do not only involve NO but also an endothelium-derived hyperpolarization (EDH)-type component mediated by stimulation of IK_{Ca} channels in endothelial cells (Rodríguez et al., 2020, 2021). However, it is unlikely that this non-NO, non-prostanoid, EDH component accounts for the defective AMPK-mediated relaxations, because it is augmented to compensate for endothelial NO impairment in renal arteries in obesity (Muñoz et al., 2020). Therefore, our findings demonstrate that endothelial dysfunction due to impaired PI3K/Akt/eNOS pathway is associated with defective AMPK-vasodilation in preglomerular arteries of genetically obese rats, as earlier reported for large conductance arteries (such as aorta) from diet-induced models of obesity (García-Prieto, Hernández-Nuño, et al., 2015). In contrast to the blunted endothelial relaxations involving NO, renal AMPK endothelium-independent vasodilation was preserved or even enhanced in OZR, as shown by the larger relaxations induced by the AMPK activator A769662 in endothelium-denuded, preglomerular arteries or arteries treated with inhibitors of NOS or PI3K in OZR. AMPK is expressed in both endothelial and vascular smooth muscle (VSM) cells in renal arteries and can activate **K_{ATP} channels** and phosphorylate the **SERCA** pump in VSM thus contributing to arterial relaxation and to the metabolic regulation of renal blood flow (Rodríguez et al., 2020, 2021). The preserved endothelium-independent relaxations elicited by A769662 in arteries from OZR suggests a therapeutic potential of AMPK activators in vascular complications of metabolic disease, where endothelium dysfunction and alterations in the eNOS/NO signalling pathway reduce NO availability.

Interestingly, our results confirm the key role of AMPK in kidney vascular function and demonstrate that AMPK activation ameliorates renal endothelial dysfunction in preglomerular arteries in obesity. Acute ex vivo treatment of whole arteries with A769662 augmented ACC phosphorylation and markedly enhanced eNOS activity and expression in LZR, thus supporting the involvement of the endothelial PI3K/Akt/NO pathway in AMPK-mediated renal vasodilation (Levine et al., 2007). In preglomerular arteries of obese rats, A769662 restored impaired endothelium-dependent relaxations by enhancing NOS expression. AMPK activation is also involved in the EDH-mediated relaxations of resistance arteries, because this EDH type vasodilation is lost after specific knockout of the endothelial AMPKα1 subunit (Enkhjargal et al., 2014). Therefore, stimulation of endothelial IK_{Ca} channels and of the EDH-type response, as recently reported in intrarenal arteries (Rodríguez et al., 2020, 2021), could also contribute to the A769662-induced restoration of endothelium-dependent relaxations in intrarenal arteries from obese rats. The beneficial effects of AMPK activation on renal endothelial dysfunction in the obese kidney were further assessed by in vivo administration of A769662 in the *ob/ob* model of genetic obesity/metabolic syndrome. We provide evidence here for endothelial dysfunction and abnormal β-adrenoceptor- and AMPK-mediated relaxations in preglomerular interlobar arteries of genetically obese mice, as shown by the impaired relaxations to ACh, isoprenaline and A769662. Interestingly, augmented eNOS phosphorylation and expression were found in renal cortex samples (including arterioles, glomeruli and peritubular capillaries) from the same animals, implying a compensatory up-regulation of NOS activity to protect glomerular NO-mediated endothelial function in the kidneys of *ob/ob* mice. Moreover, a metabolic protection was also found in renal cortex of obese kidneys, as shown by the augmented AMPK and ACC phosphorylation indicative of a higher basal AMPK activity. This could reflect a compensation for the obesity-driven fatty acid oversupply and accumulation in renal tubular and endothelial cells, in an attempt to increase ACC-mediated fatty acid incorporation and β-oxidation in the mitochondria, as reported for obese human skeletal myocytes (Green, Pedersen, et al., 2011).

In the present study, AMPK activation via in vivo administration of A769662 improved metabolic state and reduced plasma glucose levels, daily food intake and kidney weight, but also prevented inflammation and notably ameliorated kidney vascular dysfunction in obese animals. Thus, endothelium-dependent relaxations to ACh were restored to levels in lean rats and those to the β-adrenoceptor agonist isoprenaline were improved in preglomerular interlobar arteries after in vivo administration of A769662 in *ob/ob* mice, whereas basal AMPK activity was further enhanced in samples of renal cortex. The beneficial effects of AMPK activation on renal vascular function of obese kidney are consistent with the cardiovascular protective actions of drugs used in the treatment of metabolic disorders that activate AMPK such as AICAR, **metformin** or **thiazolidinediones** (Ewart & Kennedy, 2011).

Obesity-related kidney injury has been associated with renal inflammation and oxidative stress that are ameliorated by AMPK activation in diet-induced models of obesity (Decleves et al., 2011, 2014). In obesity, metabolic unbalance favours a chronic low-grade inflammation and fatty acid accumulation increases circulating levels of proinflammatory cytokines such as TNF-α, via activation of the transcription factor NFκB, and impairs insulin signalling in skeletal muscle, adipose tissue and endothelial cells (Green, Macrae, et al., 2011; McLaughlin et al., 2008; Prieto et al., 2014; Weisberg et al., 2003). TNF-α has in turn been involved in the inhibition of AMPK activity in skeletal muscle in obesity through the TNF receptor 1, suppressing fatty acid oxidation and promoting insulin resistance (Steinberg et al., 2006). The present findings demonstrate

an inflammatory response in the kidney of genetically obese mice with increased renal levels of TNF-α associated with activation of the NF-κB signalling pathway, as shown by the enhanced phosphorylation of IKK which allows NF-κB translocation into the nucleus and its activation (Hinz et al., 2012). In vivo administration of the thienopyridone A769662 attenuated renal inflammation in *ob/ob* renal cortex by suppressing NF-κB signalling (reduced IKK phosphorylation and NF-κB expression) leading to decreased levels of the inflammatory cytokine TNF-α. These findings support the modulatory role of AMPK activators such as AICAR and metformin in inflammation, as demonstrated in other cells types such as glial (Giri et al., 2004), endothelial cells (Katerelos et al., 2010) and skeletal myocytes of obese/Type 2 diabetic patients (Green, Pedersen, et al., 2011) and are consistent with the anti-inflammatory effect earlier reported for AICAR in the kidney of HFD-obese mice (Decleves et al., 2011; Decleves, Sharma & Satriano, 2014). Moreover, previous studies have shown that AMPK activation exerts its vasoprotective effects not only through augmentation of endothelial NO availability but also through its anti-inflammatory effects on endothelial cells by suppressing NF-κB, TNF-α and adhesion molecules, such as **VCAM**-1 and E-selectin (Hattori et al., 2010; Krasner et al., 2014). Accordingly, suppression of the NF-κB signalling found in renal cortex samples of *ob/ob* mice after in vivo administration of A769662 could be ascribed in part to its anti-inflammatory action on the glomerular endothelium.

ROS overproduction and oxidative stress have consistently been involved in the pathogenesis of diabetes and obesity-related vascular complications including diabetic nephropathy (Decleves et al., 2011; Jha et al., 2014; Muñoz et al., 2015, 2020; Sharma, 2016). We demonstrate here that the overall NADPH-dependent superoxide production was markedly reduced in the renal cortex of *ob/ob* mice compared with controls, and this was also the case for superoxide production in the heart of the same animals, even though cardiac ROS levels in lean animals were significantly lower than those in kidney. Reduced renal superoxide production in *ob/ob* mice is consistent with the lower levels of both basal and NADPH-dependent H_2O_2 generation recently observed in the renal cortex of the obese Zucker rat (Muñoz et al., 2020). These findings in rodent models of genetic obesity are in agreement with those first reported by the Sharma's group in the diabetic kidney (Dugan et al., 2013), where AMPK dysregulation decreased superoxide production in mitochondria that was ascribed to impaired electron transport chain activity. Mitochondria are a major source of ROS generation and provide 80% of endogenously produced basal superoxide. Fatty acid oxidation is a preferred energy source in highly metabolic cells, such as cardiac myocytes and proximal tubule renal cells. The mitochondrial β-oxidation of fatty acids accounts for two thirds of the overall kidney O_2 consumption and is located mostly in the proximal tubule. Therefore, reduced superoxide production in the kidney of rodent models of diabetes (Dugan et al., 2013; Sharma, 2016) and obesity, as shown in the present study, might reflect mitochondrial dysfunction linked to impaired fatty acid metabolism, which has also been demonstrated to underlie tubulointerstitial fibrosis in the human kidney (Kang et al., 2015).

Renal lipotoxicity and defective fatty acid oxidation caused by lipid accumulation and the associated kidney damage in obesity is related to the reduced AMPK activity (Decleves et al., 2011, 2014; Szeto et al., 2016). In our study, activation of AMPK by in vivo treatment with A769662 restored superoxide production in renal cortex but not in the heart of *ob/ob* mice, and enhanced AMPK and ACC activity. By phosphorylating and inhibiting ACC, AMPK decreases lipid synthesis and increases the import of fatty acids by the mitochondria for β-oxidation. This would suggest that AMPK treatment restores mitochondrial function and redox balance in the kidney of obese mice, in agreement with that earlier reported for the diabetic kidney where activation of AMPK with AICAR enhanced superoxide generation by improving activity of complexes I and III and mitochondrial biogenesis (Dugan et al., 2013), leading to amelioration of inflammation, fibrosis and albuminuria (Decleves et al., 2011; Declèves & Sharma, 2015; Dugan et al., 2013).

In contrast to the lower superoxide levels found in renal tubular tissues of *ob/ob* mice, ROS overproduction has been reported in mesangial cells and vascular tissues of obese and diabetic kidneys, where various sources of ROS generation including **COX-2**, **xanthine oxidase** and **Nox** have been involved in oxidative stress (Elmarakby & Imig, 2010; Jha et al., 2014; Muñoz et al., 2015, 2020). Accordingly, the overall NADPH-dependent superoxide production was confirmed to be greatly augmented in preglomerular arteries of obese rats as earlier reported (Muñoz et al., 2015, 2018), and both ex vivo and in vivo activation of AMPK were found to reduce vascular oxidative stress. AMPK reduces **Nox4** expression in podocytes (Sharma et al., 2008) and modulates redox balance in kidney preglomerular arteries through both down-regulation of Nox4 expression and through inhibition of **Nox2** activation (Rodríguez et al., 2020, 2021). The powerful suppression of superoxide production induced by ex vivo treatment with the AMPK activator A769662 in whole renal preglomerular arteries of OZR could mainly be ascribed to inhibition of Nox2, that generates superoxide, rather than down-regulation of Nox4. Thus, arterial oxidative stress in the kidney of obese rats was mostly due to augmented superoxide generation by **Nox1** and Nox2 activity, in contrast to renal cortex wherein Nox-derived superoxide was mainly produced by **Nox1**, and both expression and activity of **Nox2** were reduced in obese animals (Muñoz et al., 2020). Moreover, Nox2 up-regulation and endothelial dysfunction mediated by enhanced NF-κB activation have been shown to be reversed by AICAR in endothelial cells of AMPKα1 knockout mice (Wang et al., 2010; Schuhmacher et al., 2011). In contrast, Nox4 expression and Nox4-derived H_2O_2 production were reduced in vascular tissues of genetically obese rats (Muñoz et al., 2020) and also in hyperglycaemic Type I diabetic mice and other models of chronic kidney disease (Babelova et al., 2012; Sáenz-Medina et al., 2019). The present findings confirm that Nox4 protein content was markedly reduced in both renal cortex of *ob/ob* mice and in preglomerular arteries of OZR kidney along with reduced NADPH-dependent H_2O_2 generation and lower inhibitory effects of A769662 on H_2O_2 levels. Therefore, the powerful suppression

of ROS production induced by A769662 in whole arteries ex vivo could be mostly ascribed to Nox2 rather than Nox4 inhibition and was associated with the restoration of endothelium-dependent relaxation. Here, the beneficial effects of A769662 in ameliorating vascular oxidative stress and endothelial dysfunction in the obese kidney, and the therapeutic antioxidant potential of vascular AMPK activation were further supported by the decreased levels of NADPH-derived superoxide in renal arteries of OZR after in vivo treatment with A769662.

In conclusion, our findings provide evidence for endothelial dysfunction involving impaired AMPK-vasodilation and endothelial PI3K/Akt/eNOS pathway associated with inflammation, vascular oxidative stress and abnormal cortical redox balance in the kidney of genetic models of obesity. This suggests that vascular abnormalities and impaired vascular AMPK activity might contribute, along with glomerulopathy, interstitial fibrosis and tubular injury, to albuminuria and renal dysfunction in obesity. Activation of the energy sensor AMPK with A769662 improved the metabolic state and reduced food-intake, but notably ameliorated vascular dysfunction, oxidative stress and inflammation and also restored cortical redox balance in the obese kidney. These findings suggest that drugs activating AMPK that have been used in the treatment of metabolic disorders, may considerably improve renal vascular function and therefore represent valuable therapeutic tools to prevent obesity-related kidney injury.

ACKNOWLEDGEMENTS

This work was supported by Ministerio de Ciencia e Innovación (Spain) co-funded by the FEDER Program of EU (grants no. PID2019-105689RB and RTI2018-101840-B-I00) and by Ministerio de Economía y Competitividad (Spain) (grant no SAF2016-77526-R). Claudia Rodríguez was supported by grant FPU16/04582 from MECD (Spain). We thank Francisco Puente and Manuel Perales for expert technical assistance.

CONFLICT OF INTERESTS

All authors declare no conflict of interests.

AUTHOR CONTRIBUTIONS

D.P., C.C. and C.R. conceived the idea and designed the study. C.R., C.C., A.S. and M.M. conducted the experiments and analysed data. C.R. and D.P. wrote the manuscript. C.C., J.S.-M., M.H., M.L. and L.R. contributed to the discussion. C.R., L.R., M.L., C.C. and D.P. have read and approved the manuscript.

DECLARATION OF TRANSPARENCY AND SCIENTIFIC RIGOUR

This Declaration acknowledges that this paper adheres to the principles for transparent reporting and scientific rigour of preclinical research as stated in the BJP guidelines for Design & Analysis, Immunoblotting and Immunochemistry, and Animal Experimentation, and as recommended by funding agencies, publishers, and other organizations engaged with supporting research.

DATA AVAILABILITY STATEMENT

All data generated or analysed during this study are included in this published article (and its supplementary information files).

ORCID

Dolores Prieto https://orcid.org/0000-0001-7049-5991

REFERENCES

Abrass, C. K. (2004). Overview: Obesity: What does it have to do with kidney disease? *Journal of the American Society of Nephrology*, *15*, 2768–2772. https://doi.org/10.1097/01.ASN.0000141963.04540.3E

Alexander, S. P. H., Fabbro, D., Kelly, E., Mathie, A., Peters, J. A., Veale, E. L., Armstrong, J. F., Faccenda, E., Harding, S. D., Pawson, A. J., Sharman, J. L., Southan, C., Davies, J. A., & CGTP Collaborators. (2019). THE CONCISE GUIDE TO PHARMACOLOGY 2019/20: Enzymes. *British Journal of Pharmacology*, *176*, S297–S396. https://doi.org/10.1111/bph.14752

Alexander, S. P. H., Kelly, E., Mathie, A., Peters, J. A., Veale, E. L., Armstrong, J. F., Faccenda, E., Harding, S. D., Pawson, A. J., Sharman, J. L., Southan, C., Davies, J. A., & CGTP Collaborators. (2019). THE CONCISE GUIDE TO PHARMACOLOGY 2019/20: Transporters. *British Journal of Pharmacology*, *176*, S397–S493. https://doi.org/10.1111/bph.14753

Alexander, S. P. H., Mathie, A., Peters, J. A., Veale, E. L., Striessnig, J., Kelly, E., Armstrong, J. F., Faccenda, E., Harding, S. D., Pawson, A. J., Sharman, J. L., Southan, C., Davies, J. A., & CGTP Collaborators. (2019). THE CONCISE GUIDE TO PHARMACOLOGY 2019/20: Ion channels. *British Journal of Pharmacology*, *176*, S142–S228. https://doi.org/10.1111/bph.14749

Amann, K., & Benz, K. (2013). Structural renal changes in obesity and diabetes. *Seminars in Nephrology*, *33*, 23–33. https://doi.org/10.1016/j.semnephrol.2012.12.003

Babelova, A., Avaniadi, D., Jung, O., Fork, C., Beckmann, J., Kosowski, J., Weissmann, N., Anilkumar, N., Shah, A. M., Schaefer, L., Schröder, K., & Brandes, R. P. (2012). Role of Nox4 in murine models of kidney disease. *Free Radical Biology & Medicine*, *53*, 842–853. https://doi.org/10.1016/j.freeradbiomed.2012.06.027

Banquet, S., Delannoy, E., Agouni, A., Dessy, C., Lacomme, S., Hubert, F., Richard, V., Muller, B., & Leblais, V. (2011). Role of G(i/o)-Src kinase-PI3K/Akt pathway and caveolin-1 in β_2-adrenoceptor coupling to endothelial NO synthase in mouse pulmonary artery. *Cellular Signalling*, *23*, 1136–1143. https://doi.org/10.1016/j.cellsig.2011.02.008

Calvert, J. W., Gundewar, S., Jha, S., Greer, J. J. M., Bestermann, W. H., Tian, R., & Lefer, D. J. (2008). Acute metformin therapy confers cardioprotection against myocardial infarction via AMPK-eNOS-mediated signaling. *Diabetes*, *57*, 696–705. https://doi.org/10.2337/db07-1098

Chruscinski, A., Brede, M. E., Meinel, L., Lohse, M. J., Kobilka, B. K., & Hein, L. (2001). Differential distribution of beta-adrenergic receptor subtypes in blood vessels of knockout mice lacking beta(1)- or beta(2)-adrenergic receptors. *Molecular Pharmacology*, *60*, 955–962. https://doi.org/10.1124/mol.60.5.955

Contreras, C., Gonzalez-Garcia, I., Seoane-Collazo, P., Martinez-Sanchez, N., Linares-Pose, L., Rial-Pensado, E., Fernø, J., Tena-Sempere, M., Casals, N., Diéguez, C., & Nogueiras, R. (2017). Reduction of hypothalamic endoplasmic reticulum stress activates browning of white fat and ameliorates obesity. *Diabetes*, *66*, 87–99. https://doi.org/10.2337/db15-1547

Cool, B., Zinker, B., Chiou, W., Kifle, L., Cao, N., Perham, M., Dickinson, R., Adler, A., Gagne, G., Iyengar, R., Zhao, G., Marsh, K., Kym, P., Jung, P., Camp, H. S., & Frevert, E. (2006). Identification and characterization of a small molecule AMPK activator that treats key components of type

2 diabetes and the metabolic syndrome. *Cell Metabolism*, *3*, 403–416. https://doi.org/10.1016/j.cmet.2006.05.005

Curtis, M. J., Alexander, S. P. H., Cirino, G., Docherty, J. R., George, C. H., Giembycz, M. A., Hoyer, D., Insel, P. A., Izzo, A. A., Ji, Y., MacEwan, D. J., Sobey, C. G., Stanford, S. C., Teixeira, M. M., Wonnacott, S., & Ahluwalia, A. (2018). Experimental design and analysis and their reporting II: updated and simplified guidance for authors and peer reviewers. *British Journal of Pharmacology*, *175*, 987–993. https://doi.org/10.1111/bph.14153

De Vries, A. P. J., Ruggenenti, P., Ruan, X. Z., Praga, M., Cruzado, J. M., Bajema, I. M., D'Agati, V., Lamb, H. J., Barlovic, D. P., Hojs, R., & Abbate, M. (2014). Fatty kidney: Emerging role of ectopic lipid in obesity-related renal disease. *The Lancet Diabetes and Endocrinology*, *2*, 417–426. https://doi.org/10.1016/S2213-8587(14)70065-8

Declèves, A. E., & Sharma, K. (2015). Obesity and kidney disease: Differential effects of obesity on adipose tissue and kidney inflammation and fibrosis. *Current Opinion in Nephrology and Hypertension*, *24*, 28–36. https://doi.org/10.1097/MNH.0000000000000087

Declèves, A. E., Zolkipli, Z., Satriano, J., Wang, L., Nakayama, T., Rogac, M., Le TP, N. J. L., Farquhar, M. G., Naviaux, R. K., & Sharma, K. (2014). Regulation of lipid accumulation by AMP-activated kinase [corrected] in high fat diet-induced kidney injury. *Kidney International*, *85*, 611–623. https://doi.org/10.1038/ki.2013.462

Declèves, A. E., Mathew, A. V., Cunard, R., & Sharma, K. (2011). AMPK mediates the initiation of kidney disease induced by a high-fat diet. *Journal of the American Society of Nephrology*, *22*, 1846–1855. https://doi.org/10.1681/ASN.2011010026

Deng, G., Long, Y., Yu, Y. R., & Li, M. R. (2010). Adiponectin directly improves endothelial dysfunction in obese rats through the AMPK-eNOS pathway. *International Journal of Obesity*, *34*, 165–171. https://doi.org/10.1038/ijo.2009.205

Dugan, L. L., You, Y. H., Ali, S. S., Diamond-Stanic, M., Miyamoto, S., DeCleves, A. E., Andreyev, A., Quach, T., Ly, S., Shekhtman, G., & Nguyen, W. (2013). AMPK dysregulation promotes diabetes-related reduction of superoxide and mitochondrial function. *The Journal of Clinical Investigation*, *123*, 4888–4899. https://doi.org/10.1172/JCI66218

Elmarakby, A. A., & Imig, J. D. (2010). Obesity is the major contributor to vascular dysfunction and inflammation in high-fat diet hypertensive rats. *Clinical Science (London, England)*, *118*, 291–301. https://doi.org/10.1042/CS20090395

Enkhjargal, B., Godo, S., Sawada, A., Suvd, N., Saito, H., Noda, K., Satoh, K., & Shimokawa, H. (2014). Endothelial AMP-activated protein kinase regulates blood pressure and coronary flow responses through hyperpolarization mechanism in mice. *Arteriosclerosis, Thrombosis, and Vascular Biology*, *34*, 1505–1513. https://doi.org/10.1161/ATVBAHA.114.303735

Ewart, M. A., & Kennedy, S. (2011). AMPK and vasculoprotection. *Pharmacology & Therapeutics*, *131*, 242–253. https://doi.org/10.1016/j.pharmthera.2010.11.002

Ferro, A., Coash, M., Yamamoto, T., Rob, J., Ji, Y., & Queen, L. (2004). Nitric oxide-dependent β 2-adrenergic dilatation of rat aorta is mediated through activation of both protein kinase A and Akt. *British Journal of Pharmacology*, *143*, 397–403. https://doi.org/10.1038/sj.bjp.0705933

García-Prieto, C. F., Gil-Ortega, M., Aránguez, I., Ortiz-Besoain, M., Somoza, B., & Fernández-Alfonso, M. S. (2015). Vascular AMPK as an attractive target in the treatment of vascular complications of obesity. *Vascular Pharmacology*, *67-69*, 10–20. https://doi.org/10.1016/j.vph.2015.02.017

García-Prieto, C. F., Hernández-Nuño, F., Rio, D. D., Ruiz-Hurtado, G., Aránguez, I., Ruiz-Gayo, M., Somoza, B., & Fernández-Alfonso, M. S. (2015). High-fat diet induces endothelial dysfunction through a down-regulation of the endothelial AMPK-PI3K-Akt-eNOS pathway. *Molecular Nutrition & Food Research*, *59*, 520–532. https://doi.org/10.1002/mnfr.201400539

García-Prieto, C. F., Pulido-Olmo, H., Ruiz-Hurtado, G., Gil-Ortega, M., Aranguez, I., Rubio, M. A., Ruiz-Gayo, M., Somoza, B., & Fernández-Alfonso, M. S. (2015). Mild caloric restriction reduces blood pressure and activates endothelial AMPK-PI3K-Akt-eNOS pathway in obese Zucker rats. *Vascular Pharmacology*, *65-66*, 3–12. https://doi.org/10.1016/j.vph.2014.12.001

Giri, S., Nath, N., Smith, B., Viollet, B., Singh, A. K., & Singh, I. (2004). 5-aminoimidazole-4-carboxamide-1-beta-4-ribofuranoside inhibits proinflammatory response in glial cells: A possible role of AMP-activated protein kinase. *The Journal of Neuroscience*, *24*, 479–487. https://doi.org/10.1523/JNEUROSCI.4288-03.2004

Green, C. J., Macrae, K., Fogarty, S., Hardie, D. G., Sakamoto, K., & Hundal, H. S. (2011). Counter-modulation of fatty acid-induced pro-inflammatory nuclear factor κB signalling in rat skeletal muscle cells by AMP-activated protein kinase. *The Biochemical Journal*, *435*, 463–474. https://doi.org/10.1042/BJ20101517

Green, C. J., Pedersen, M., Pedersen, B. K., & Scheele, C. (2011). Elevated NF-κB activation is conserved in human myocytes cultured from obese type 2 diabetic patients and attenuated by AMP-activated protein kinase. *Diabetes*, *60*, 2810–2819. https://doi.org/10.2337/db11-0263

Hallows, K. R., Mount, P. F., Pastor-Soler, N. M., & Power, D. A. (2010). Role of the energy sensor AMP-activated protein kinase in renal physiology and disease. *American Journal of Physiology. Renal Physiology*, *298*, F1067–F1077. https://doi.org/10.1152/ajprenal.00005.2010

Hattori, Y., Jojima, T., Tomizawa, A., Satoh, H., Hattori, S., Kasai, K., & Hayashi, T. (2010). A glucagon-like peptide-1 (GLP-1) analogue, liraglutide, upregulates nitric oxide production and exerts anti-inflammatory action in endothelial cells. *Diabetologia*, *53*, 2256–2263. https://doi.org/10.1007/s00125-010-1831-8

Hinz, M., Arslan, S., & Scheidereit, C. (2012). It takes two to tango: IκBs, the multifunctional partners of NF-κB. *Immunological Reviews*, *246*, 59–76. https://doi.org/10.1111/j.1600-065X.2012.01102.x

Ix, J. H., & Sharma, K. (2010). Mechanisms linking obesity, chronic kidney disease, and fatty liver disease: The roles of fetuin-a, adiponectin, and AMPK. *Journal of the American Society of Nephrology*, *21*, 406–412. https://doi.org/10.1681/ASN.2009080820

Jha, J. C., Gray, S. P., Barit, D., Okabe, J., El-Osta, A., Namikoshi, T., Thallas-Bonke, V., Wingler, K., Szyndralewiez, C., Heitz, F., & Touyz, R. M. (2014). Genetic targeting or pharmacologic inhibition of NADPH oxidase Nox4 provides renoprotection in long-term diabetic nephropathy. *Journal of the American Society of Nephrology: JASN*, *25*, 1237–1254. https://doi.org/10.1681/ASN.2013070810

Kang, H. M., Ahn, S. H., Choi, P., Ko, Y. A., Han, S. H., Chinga, F., Park, A. S. D., Tao, J., Sharma, K., Pullman, J., Bottinger, E. P., Goldberg, I. J., & Susztak, K. (2015). Defective fatty acid oxidation in renal tubular epithelial cells has a key role in kidney fibrosis development. *Nature Medicine*, *21*, 37–46. https://doi.org/10.1038/nm.3762

Katerelos, M., Mudge, S., Stapleton, D., Auwardt, R., Fraser, S., Chen, C. G., Kemp, B. E., & Power, D. A. (2010). 5-aminoimidazole-4-carboxamide ribonucleoside and AMP-activated protein kinase inhibit signalling through NF-kB. *Immunology and Cell Biology*, *88*, 754–760. https://doi.org/10.1038/icb.2010.44

Kou, R., & Michel, T. (2007). Epinephrine regulation of the endothelial nitric-oxide synthase: Roles of RAC1 and beta3-adrenergic receptors in endothelial NO signaling. *The Journal of Biological Chemistry*, *282*, 32719–32729. https://doi.org/10.1074/jbc.M706815200

Kramer, H., Luke, A., Bidani, A., Cao, G., Cooper, R., & McGee, D. (2005). Obesity and prevalent and incident CKD: The hypertension detection and follow-up program. *American Journal of Kidney Diseases*, *46*, 587–594. https://doi.org/10.1053/j.ajkd.2005.06.007

Krasner, N. M., Ido, Y., Ruderman, N. B., & Cacicedo, J. M. (2014). Glucagon-like peptide-1 (GLP-1) analog liraglutide inhibits endothelial cell inflammation through a calcium and AMPK dependent

mechanism. *PLoS ONE*, *9*, e97554. https://doi.org/10.1371/journal.pone.0097554

Kume, S., Uzu, T., S-i, A., Sugimoto, T., Isshiki, K., Chin-Kanasaki, M., Sakaguchi, M., Kubota, N., Terauchi, Y., Kadowaki, T., & Haneda, M. (2007). Role of altered renal lipid metabolism in the development of renal injury induced by a high-fat diet. *Journal of the American Society of Nephrology*, *18*, 2715–2723. https://doi.org/10.1681/ASN.2007010089

Lee, W. J., Lee, I. K., Kim, H. S., Kim, Y. M., Koh, E. H., Won, J. C., Han, S. M., Kim, M. S., Jo, I., Oh, G. T., Park, I. S., Youn, J. H., Park, S. W., Lee, K. U., & Park, J. Y. (2005). α-Lipoic acid prevents endothelial dysfunction in obese rats via activation of AMP-activated protein kinase. *Arteriosclerosis, Thrombosis, and Vascular Biology*, *25*, 2488–2494. https://doi.org/10.1161/01.ATV.0000190667.33224.4c

Levine, Y. C., Li, G. K., & Michel, T. (2007). Agonist-modulated regulation of AMP-activated protein kinase (AMPK) in endothelial cells. Evidence for an AMPK -> Rac1 -> Akt -> endothelial nitric-oxide synthase pathway. *The Journal of Biological Chemistry*, *282*, 20351–20364. https://doi.org/10.1074/jbc.M702182200

Lilley, E., Stanford, S. C., Kendall, D. E., Alexander, S. P., Cirino, G., Docherty, J. R., George, C. H., Insel, P. A., Izzo, A. A., Ji, Y., Panettieri, R. A., Sobey, C. G., Stefanska, B., Stephens, G., Teixeira, M., & Ahluwalia, A. (2020). ARRIVE 2.0 and the British Journal of Pharmacology: Updated guidance for 2020. *British Journal of Pharmacology*, *177*(16), 3611–3616. https://doi.org/10.1111/bph.15178

Liu, Y., Wan, Q., Guan, Q., Gao, L., & Zhao, J. (2005). High-fat diet feeding impairs both the expression and activity of AMPKa in rats' skeletal muscle. *Biochemical and Biophysical Research Communications*, *339*, 701–707.

Lobato, N. S., Filgueira, F. P., Prakash, R., Giachini, F. R., Ergul, A., Carvalho, M. H. C., Webb, R. C., Tostes, R. C., & Fortes, Z. B. (2013). Reduced endothelium-dependent relaxation to anandamide in mesenteric arteries from young obese Zucker rats. *PLoS ONE*, *8*, e63449. https://doi.org/10.1371/journal.pone.0063449

Lopez, M., Nogueiras, R., Tena-Sempere, M., & Dieguez, C. (2016). Hypothalamic AMPK: A canonical regulator of whole-body energy balance. *Nature Reviews. Endocrinology*, *12*, 421–432. https://doi.org/10.1038/nrendo.2016.67

Martinez-Sanchez, N., Seoane-Collazo, P., Contreras, C., Varela, L., Villarroya, J., Rial-Pensado, E., Buqué, X., Aurrekoetxea, I., Delgado, T. C., Vázquez-Martínez, R., & González-García, I. (2017). Hypothalamic AMPK-ER stress-JNK1 Axis mediates the central actions of thyroid hormones on energy balance. *Cell Metabolism*, *26*(212–229), e212.

McLaughlin, T., Deng, A., Gonzales, O., Aillaud, M., Yee, G., Lamendola, C., Abbasi, F., Connolly, A. J., Sherman, A., Cushman, S. W., Reaven, G., & Tsao, P. S. (2008). Insulin resistance is associated with a modest increase in inflammation in subcutaneous adipose tissue of moderately obese women. *Diabetologia*, *51*, 2303–2308. https://doi.org/10.1007/s00125-008-1148-z

Motawi, T. M., Hashem, R. M., Rashed, L. A., & El-Razek, S. M. (2009). Comparative study between the effect of the peroxisome proliferator activated receptor-alpha ligands fenofibrate and n-3 polyunsaturated fatty acids on activation of 5'-AMP-activated protein kinase-alpha1 in high-fat fed rats. *The Journal of Pharmacy and Pharmacology*, *61*, 1339–1346. https://doi.org/10.1211/jpp.61.10.0010

Muñoz, M., López-Oliva, M. E., Pinilla, E., Martínez, M. P., Sánchez, A., Rodríguez, C., García-Sacristán, A., Hernández, M., Rivera, L., & Prieto, D. (2017). CYP epoxygenase-derived H_2O_2 is involved in the endothelium-derived hyperpolarization (EDH) and relaxation of intrarenal arteries. *Free Radical Biology and Medicine*, *106*, 168–183. https://doi.org/10.1016/j.freeradbiomed.2017.02.031

Muñoz, M., López-oliva, M. E., Rodríguez, C., Pilar, M., Sáenz-medina, J., Sánchez, A., Climent, B., Benedito, S., García-Sacristán, A., Rivera, L., & Hernández, M. (2020). Differential contribution of Nox1, Nox2 and Nox4 to kidney vascular oxidative stress and endothelial dysfunction in obesity. *Redox Biology*, *28*, 101330–101330. https://doi.org/10.1016/j.redox.2019.101330

Muñoz, M., Martínez, M. P., López-Oliva, M. E., Rodríguez, C., Corbacho, C., Carballido, J., García-Sacristán, A., Hernández, M., Rivera, L., Sáenz-Medina, J., & Prieto, D. (2018). Hydrogen peroxide derived from NADPH oxidase 4- and 2 contributes to the endothelium-dependent vasodilatation of intrarenal arteries. *Redox Biology*, *19*, 92–104. https://doi.org/10.1016/j.redox.2018.08.004

Muñoz, M., Sánchez, A., Pilar Martínez, M., Benedito, S., López-Oliva, M.-E., García-Sacristán, A., Hernández, M., & Prieto, D. (2015). COX-2 is involved in vascular oxidative stress and endothelial dysfunction of renal interlobar arteries from obese Zucker rats. *Free Radical Biology & Medicine*, *84*, 77–90. https://doi.org/10.1016/j.freeradbiomed.2015.03.024

Percie du Sert, N., Hurst, V., Ahluwalia, A., Alam, S., Avey, M. T., Baker, M., Browne, W. J., Clark, A., Cuthill, I. C., Dirnagl, U., Emerson, M., Garner, P., Holgate, S. T., Howells, D. W., Karp, N. A., Lazic, S. E., Lidster, K., MacCallum, C. J., Macleod, M., & Würbel, W. (2020). The ARRIVE guidelines 2.0: Updated guidelines for reporting animal research. *British journal of pharmacology*, *177*(16), 3617–3624.

Prieto, D., Contreras, C., & Sánchez, A. (2014). Endothelial dysfunction, obesity and insulin resistance. *Current Vascular Pharmacology*, *12*, 412–426. https://doi.org/10.2174/1570161112666140423221008

Rodríguez, C., Contreras, C., Sáenz-Medina, J., Muñoz, M., Corbacho, C., Carballido, J., García-Sacristán, A., Hernandez, M., López, M., Rivera, L., & Prieto, D. (2020). Activation of the AMP-related kinase (AMPK) induces renal vasodilatation and downregulates Nox-derived reactive oxygen species (ROS) generation. *Redox Biology*, *34*, 101575. https://doi.org/10.1016/j.redox.2020.101575

Rodríguez, C., Muñoz, M., Contreras, C., & Prieto, D. (2021). AMPK, metabolism and vascular function. *The FEBS Journal*, *280*(12), 3746–3771.

Rossoni, L. V., Wareing, M., Wenceslau Camilla, F., Al-Abri, M., Cobb, C., & Austin, C. (2011). Acute simvastatin increases endothelial nitric oxide synthase phosphorylation via AMP-activated protein kinase and reduces contractility of isolated rat mesenteric resistance arteries. *Clinical Science*, *121*, 449–458. https://doi.org/10.1042/CS20110259

Ruderman, N., & Prentki, M. (2004). AMP kinase and malonyl-CoA: Targets for therapy of the metabolic syndrome. *Nature Reviews. Drug Discovery*, *3*, 340–351. https://doi.org/10.1038/nrd1344

Sáenz-Medina, J., Muñoz, M., Sanchez, A., Rodriguez, C., Jorge, E., Corbacho, C., Izquierdo, D., Santos, M., Donoso, E., Virumbrales, E., & Ramil, E. (2019). Nox1-derived oxidative stress as a common pathogenic link between obesity and hyperoxaluria-related kidney injury. *Urolithiasis*, *48*, 481–492.

Salatto, C. T., Miller, R. A., Cameron, K. O., Cokorinos, E., Reyes, A., Ward, J., Calabrese, M. F., Kurumbail, R. G., Rajamohan, F., Kalgutkar, A. S., Tess, D. A., Shavnya, A., Genung, N. E., Edmonds, D. J., Jatkar, A., Maciejewski, B. S., Amaro, M., Gandhok, H., Monetti, M., … Rolph, T. (2017). Selective activation of AMPK β1-containing isoforms improves kidney function in a rat model of diabetic nephropathy. *Journal of Pharmacology and Experimental Therapeutics*, *361*, 303–311. https://doi.org/10.1124/jpet.116.237925

Schuhmacher, S., Foretz, M., Knorr, M., Jansen, T., Hortmann, M., Wenzel, P., Oelze, M., Kleschyov, A. L., Daiber, A., Keaney, J. F. Jr., Wegener, G., Lackner, K., Münzel, T., Viollet, B., & Schulz, E. (2011). α1AMP-activated protein kinase preserves endothelial function during chronic angiotensin II treatment by limiting Nox2 upregulation. *Arteriosclerosis, Thrombosis, and Vascular Biology*, *31*, 560–566. https://doi.org/10.1161/ATVBAHA.110.219543

Sharma, K. (2014). Obesity, oxidative stress, and fibrosis in chronic kidney disease. *Kidney International. Supplement*, *4*, 113–117.

Sharma, K. (2016). Obesity and diabetic kidney disease: Role of oxidant stress and redox balance. *Antioxidants & Redox Signaling*, *25*, 208–216. 10.1089/ars.2016.6696

Sharma, K., Ramachandrarao, S., Qiu, G., Usui, H. K., Zhu, Y., Dunn, S. R., Ouedraogo, R., Hough, K., McCue, P., Chan, L., Falkner, B., & Goldstein, B. J. (2008). Adiponectin regulates albuminuria and podocyte function in mice. *The Journal of Clinical Investigation*, *118*, 1645–1656. https://doi.org/10.1172/JCI32691

Steinberg, G. R., & Kemp, B. E. (2009). AMPK in health and disease. *Physiological Reviews*, *89*, 1025–1078. https://doi.org/10.1152/physrev.00011.2008

Steinberg, G. R., Michell, B. J., van Denderen, B. J., Watt, M. J., Carey, A. L., Fam, B. C., Andrikopoulos, S., Proietto, J., Görgün, C. Z., Carling, D., & Hotamisligil, G. S. (2006). Tumor necrosis factor alpha-induced skeletal muscle insulin resistance involves suppression of AMP-kinase signaling. *Cell Metabolism*, *4*, 465–474. https://doi.org/10.1016/j.cmet.2006.11.005

Sun, W., Lee, T. S., Zhu, M., Gu, C., Wang, Y., Zhu, Y., & Shyy, J. Y. J. (2006). Statins activate AMP-activated protein kinase in vitro and in vivo. *Circulation*, *114*, 2655–2662. https://doi.org/10.1161/CIRCULATIONAHA.106.630194

Szeto, H. H., Liu, S., Soong, Y., Alam, N., Prusky, G. T., & Seshan, S. V. (2016). Protection of mitochondria prevents high-fat diet–induced glomerulopathy and proximal tubular injury. *Kidney International*, *90*, 997–1011. https://doi.org/10.1016/j.kint.2016.06.013

Wang, S., Zhang, M., Liang, B., Xu, J., Xie, Z., Liu, C., Viollet, B., Yan, D., & Zou, M. H. (2010). AMPKα2 deletion causes aberrant expression and activation of NAD(P)H oxidase and consequent endothelial dysfunction in vivo: Role of 26S proteasomes. *Circulation Research*, *106*, 1117–1128. https://doi.org/10.1161/CIRCRESAHA.109.212530

Weisberg, S. P., McCann, D., Desai, M., Rosenbaum, M., Leibel, R. L., & Ferrante, A. W. Jr. (2003). Obesity is associated with macrophage accumulation in adipose tissue. *The Journal of Clinical Investigation*, *112*, 1796–1808. https://doi.org/10.1172/JCI200319246

Zhou, G., Myers, R., Li, Y., Chen, Y., Shen, X., Fenyk-Melody, J., Wu, M., Ventre, J., Doebber, T., Fujii, N., Musi, N., Hirshman, M. F., Goodyear, L. J., & Moller, D. E. (2001). Role of AMP-activated protein kinase in mechanism of metformin action. *The Journal of Clinical Investigation*, *108*, 1167–1174. https://doi.org/10.1172/JCI13505

SUPPORTING INFORMATION

Additional supporting information may be found online in the Supporting Information section at the end of this article.

How to cite this article: Rodríguez, C., Sánchez, A., Sáenz-Medina, J., Muñoz, M., Hernández, M., López, M., Rivera, L., Contreras, C., & Prieto, D. (2021). Activation of AMP kinase ameliorates kidney vascular dysfunction, oxidative stress and inflammation in rodent models of obesity. *British Journal of Pharmacology*, *178*(20), 4085–4103. https://doi.org/10.1111/bph.15600